Diffraction model for the external occulter of the solar coronagraph ASPIICS

Raphaël Rougeot

OCA, Nice – 14/05/2018

Outline

1) Proba-3 mission and ASPIICS
2) Diffraction from external occulters
   a) How to compute diffraction
   b) Diffraction patterns for several occulters
3) Penumbra profile
4) Conclusion

Proba-3 mission and ASPIICS

ESA Proba-3 mission

- In-orbit demonstration of precise **Formation Flying**
- Two spacecraft flying **150m apart**, controlled with a millimeter accuracy

Occulter Spacecraft

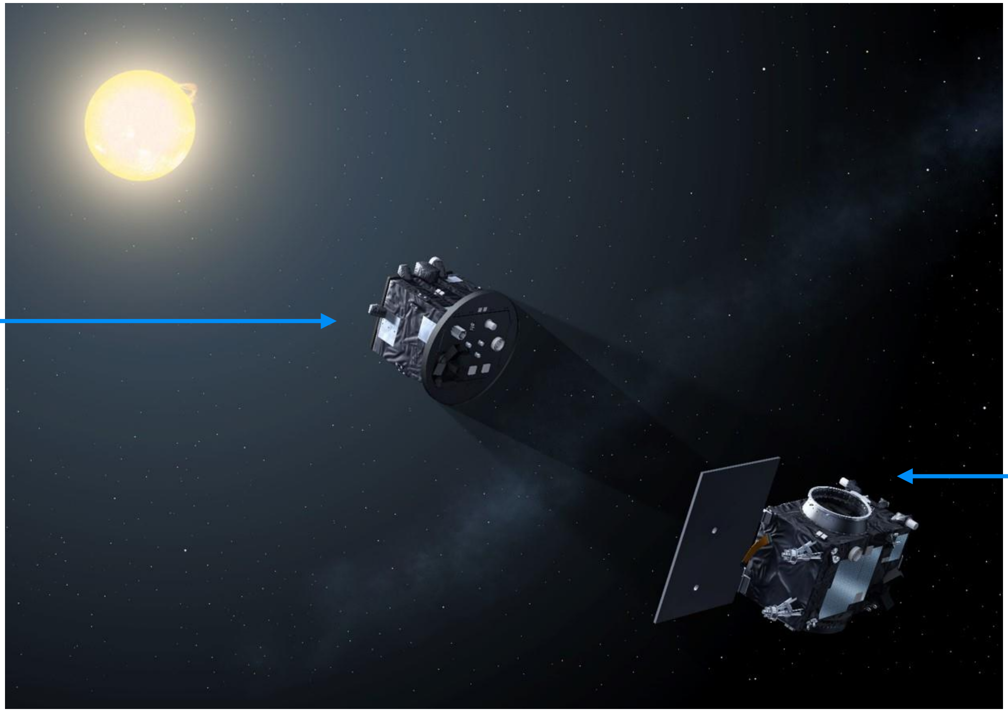

Coronagraph Spacecraft

ESA Proba-3 mission

- In-orbit demonstration of precise **Formation Flying**
- Two spacecraft flying **150m apart**, controlled with a millimeter accuracy
- The formation will be **co-aligned with the Sun** during the **6-hours** apogee phase

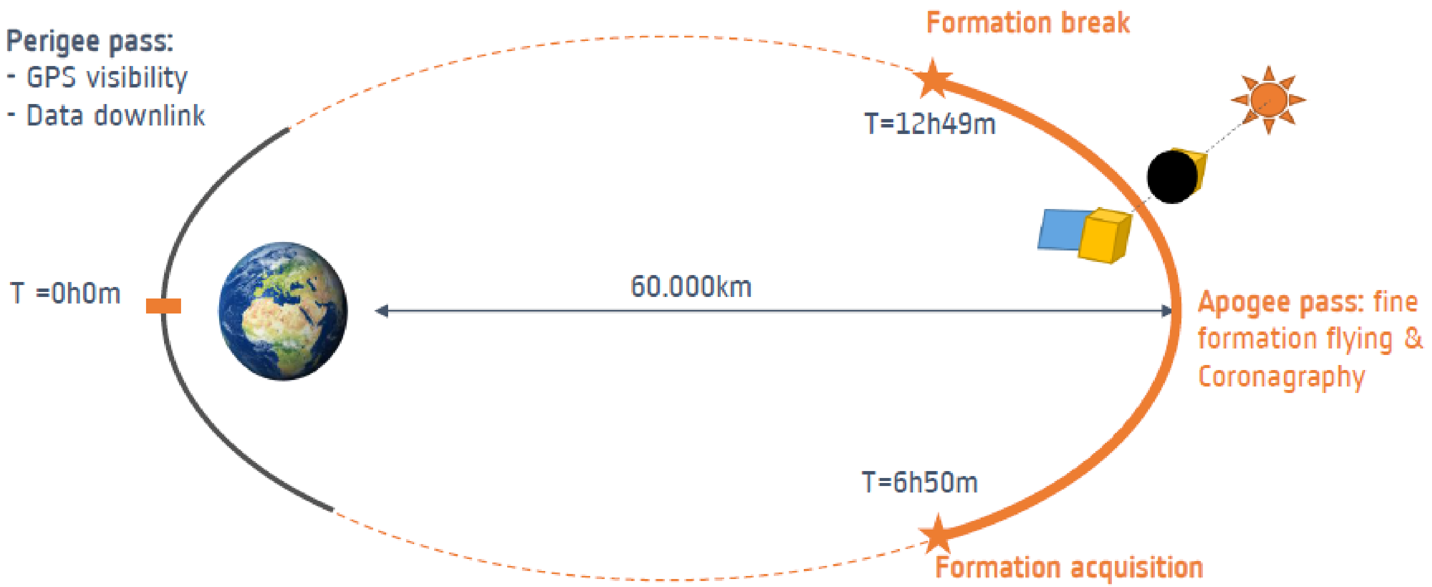

Solar coronagraph ASPIICS

- Associtation de Satellites Pour l'Imagerie et l'Interférométrie de la Couronne Solaire

- A **1,42m diameter occulting disk** carried by the Occulter Spacecraft
  A **5cm Lyot-style coronagraph** on the Coronagraph Spacecraft

- Observation of the **K-corona**
  - Findings on the heating process
  - Alven's waves, dynamics of the plasma
  - Coronal Mass Ejections

Lamy, 2010
Renotte, 2015

ASPIICS in a nutshell

White light [540nm ; 570nm]
2,8 arcsec/pixel
High cadence

Coronagraphy and diffraction

- The **corona of the sun** is much fainter than the solar disk itself
  Observation in white light requires **perfect eclipse conditions**

$$B_{corona} \sim 10^{-6} \ to \ 10^{-9} B_{sun}$$

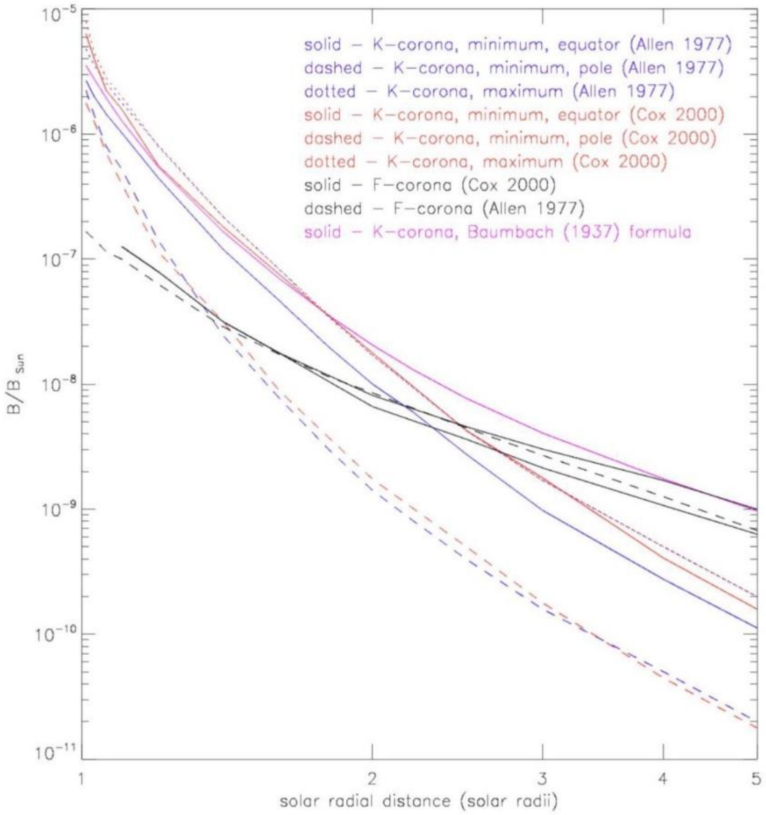

Allen, 1997
Cox, 2000

Coronagraphy and diffraction

- The hybrid externally occulted Lyot solar coronagraph ASPIICS

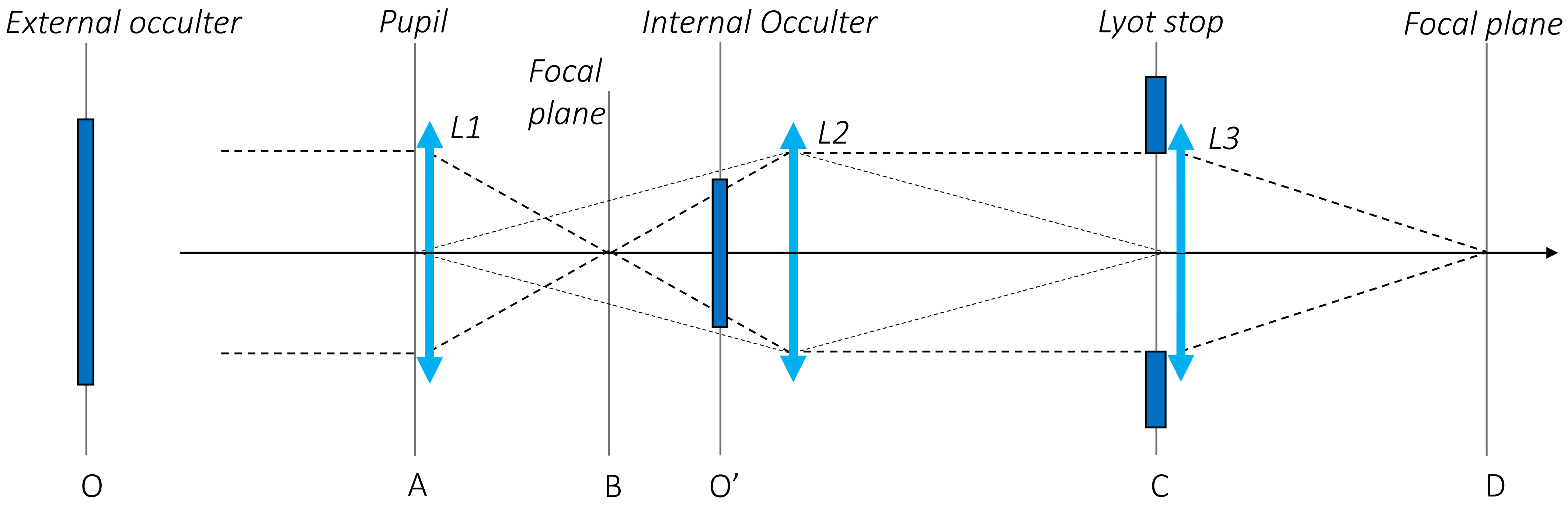

Coronagraphy and diffraction

- The hybrid externally occulted Lyot solar coronagraph ASPIICS

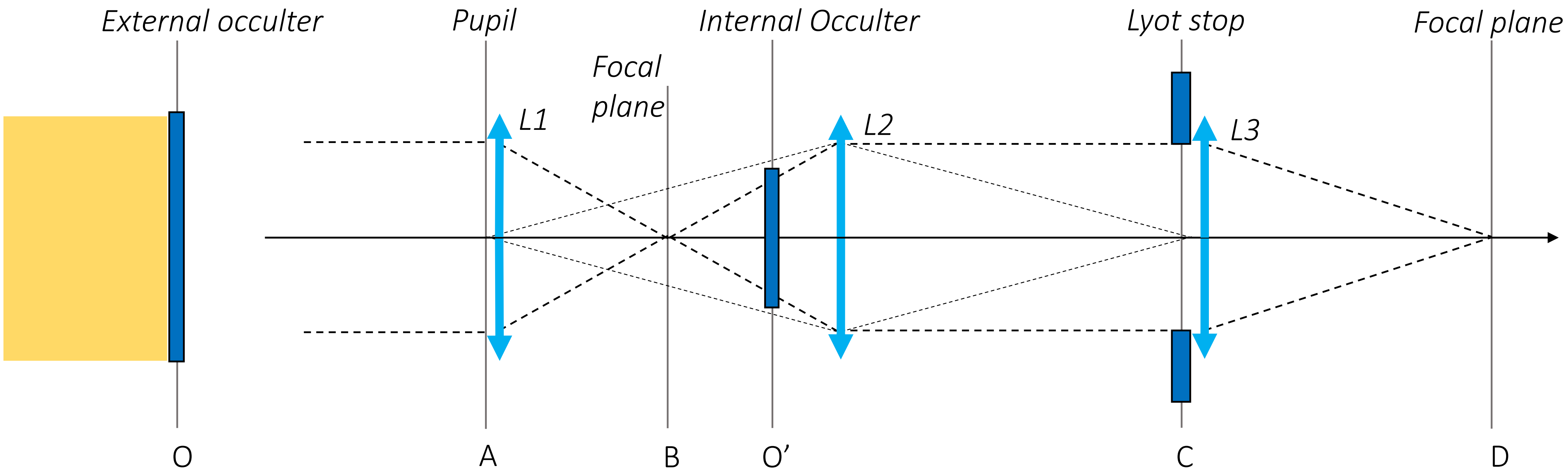

Coronagraphy and diffraction

- The hybrid externally occulted Lyot solar coronagraph ASPIICS

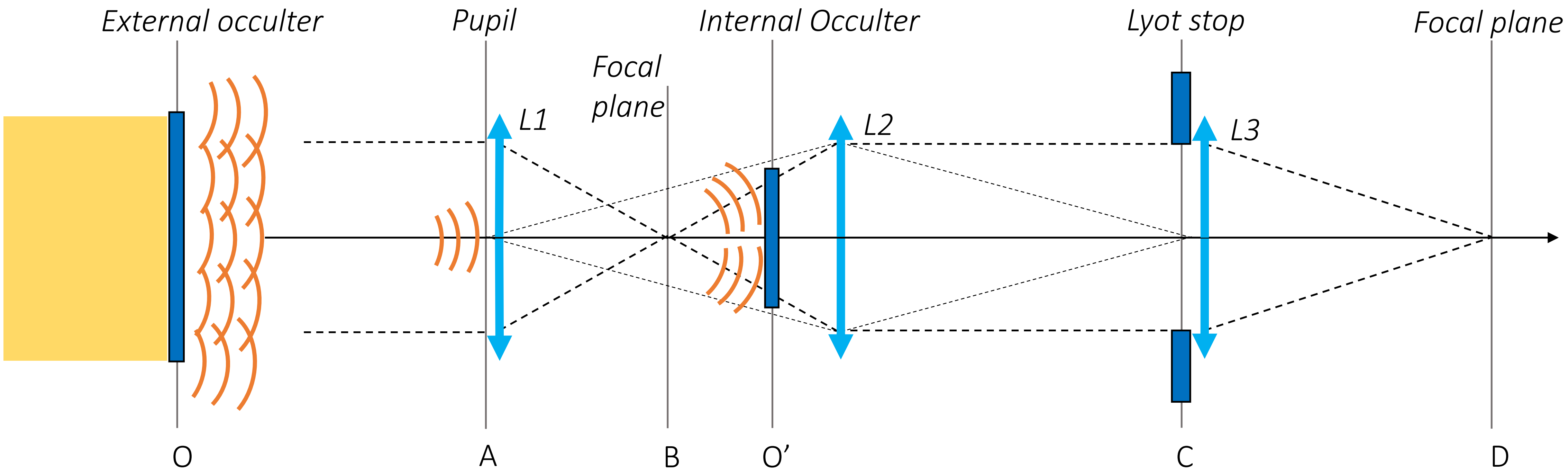

Coronagraphy and diffraction

- The hybrid externally occulted Lyot solar coronagraph ASPIICS

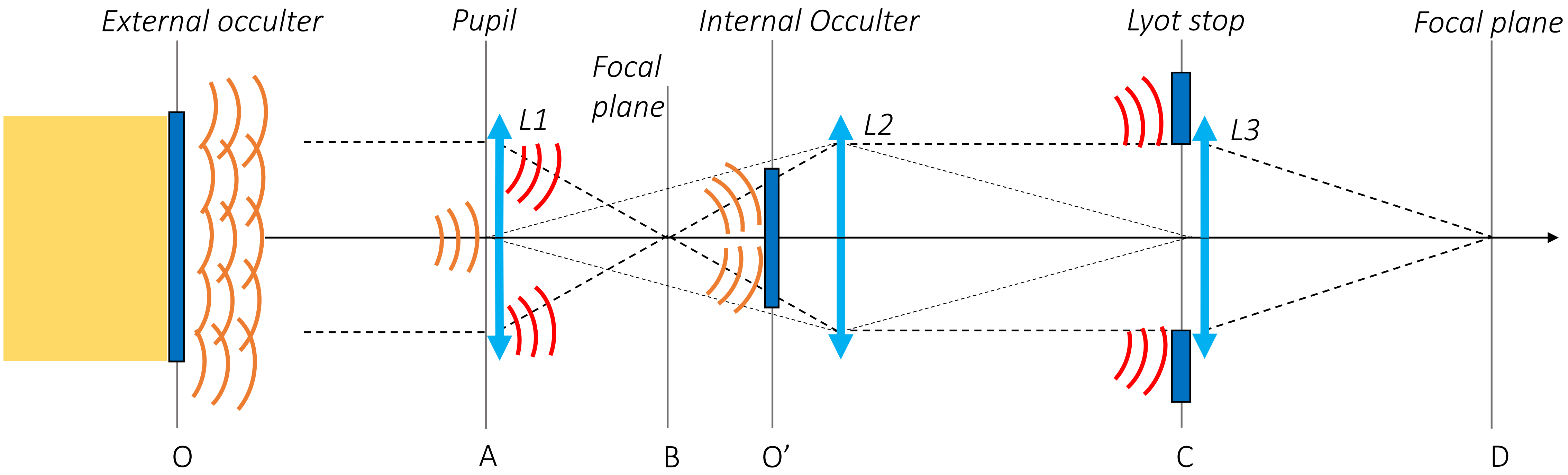

Diffraction by an external occulter

Diffraction by an external occulter

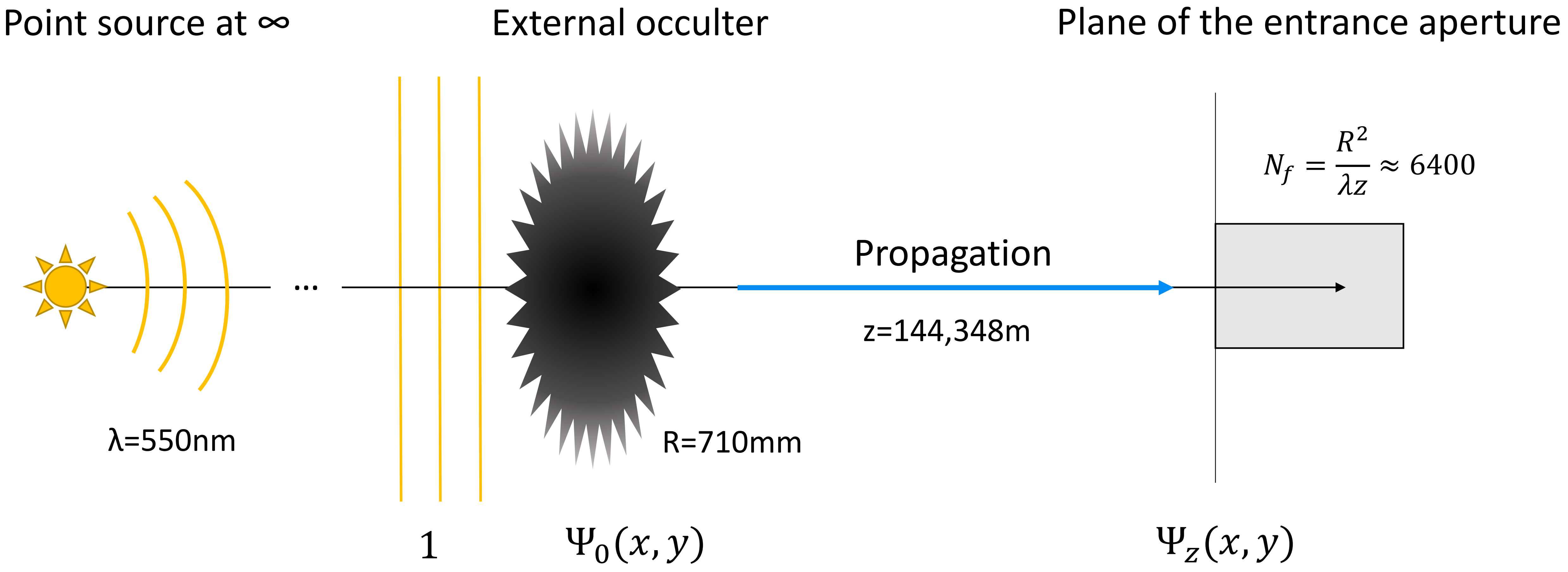

Diffraction by an external occulter

- Major issue in solar coronagraphy: the Sun is an **extended light source**

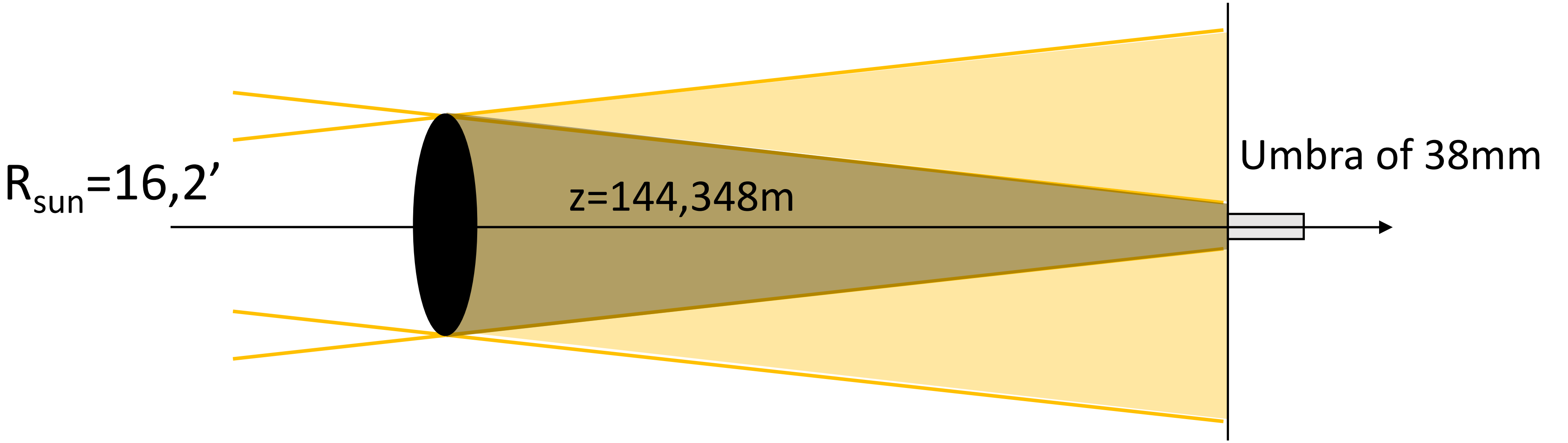

- The diffraction pattern must be known over a **large spatial extent**
  ≠ **stellar coronagraphy**

How to compute diffraction?

	Apodisation	No Axis-symmetry	
Brute force 2D FFT	√	√	*Rougeot & Aime, 2018*
Analytical Hankel transform	√	X	*Aime, 2013*
Vanderbei et al. Approach	√	O (periodicity)	*Vanderbei, 2003*
Lommel series	X	X	*Aime, 2013*
Maggi-Rubinowicz representation Boundary diffraction integral	X	√	*Cady, 2012* *Born & Wolf*

How to compute diffraction

- **Brute force 2D FFT**

The occulter is padded in a 2D arrays

$$\Psi_z(x,y) = \mathcal{F}^{-1}\left[\mathcal{F}\underbrace{[\Psi_0(x,y)]}_{\text{Occulter}} \times \underbrace{\exp(-i\pi\lambda z(u^2+v^2))}_{\text{Fresnel filter}}\right]$$

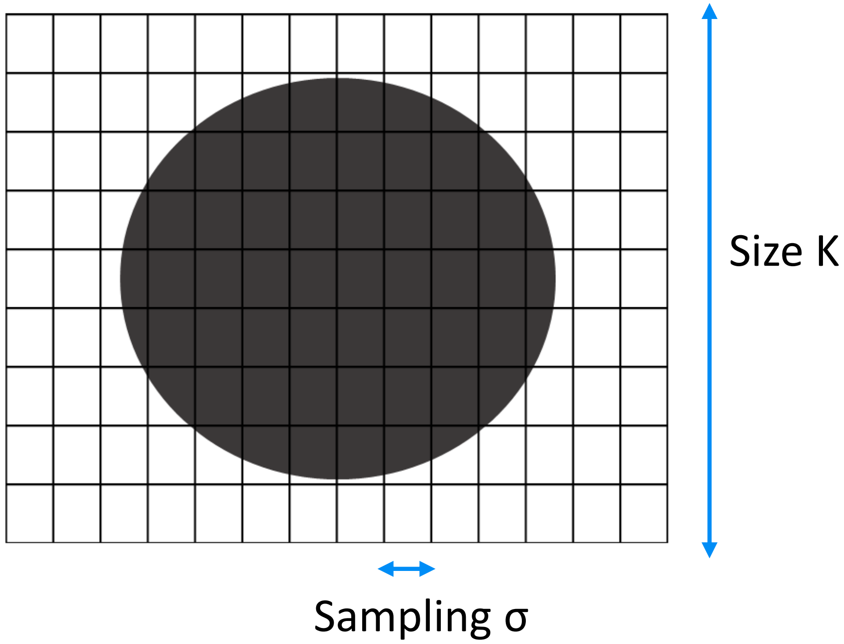

Condition from the Fresnel filter: $\sigma > \sqrt{\frac{Kz}{\lambda}}$

Consequence: **K of very large size**

In Rougeot & Aime 2018, we tried 156000 x 156000, not sufficient for petalized shape

How to compute diffraction

- **Maggi-Rubinowicz representation**

Requires a binary mask (1 or 0)

$$\Psi_z(x,y) = -\Psi_z^{(d)}(x,y) \text{ in the geometrical shadow}$$

$$\Psi_z(x,y) = \Psi_0(x,y) - \Psi_z^{(d)}(x,y) \text{ otherwise}$$

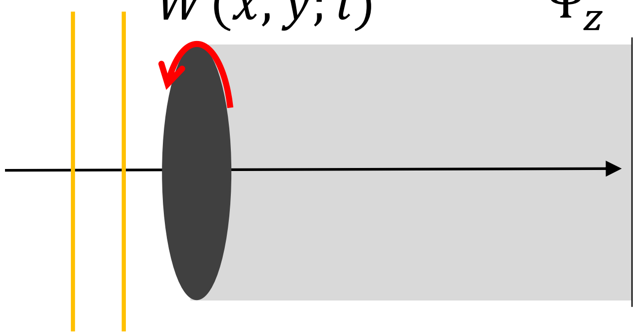

Boundary diffraction integral $\Psi_z^{(d)} = \frac{1}{4\pi}\oint_\partial W\,\vec{dl}$

Sampling of the occulter edge must be carefully chosen

Cady, 2012
Born & Wolf
Rougeot & Aime, 2018

Diffraction by an external occulter

- The **sharp-edged** occulting disk

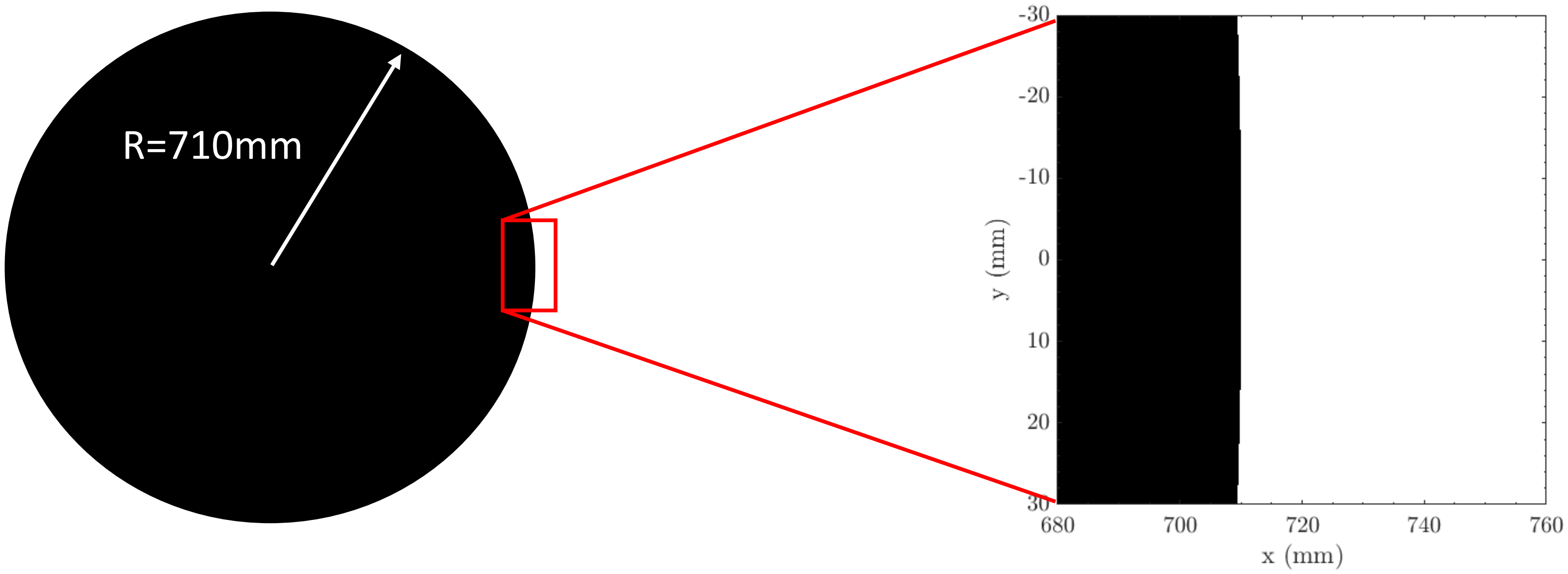

Occulting ratio of 1,05 solar radius at z=144m

Diffraction by an external occulter

- The **sharp-edged** occulting disk

The bright spot of Arago (or Poisson… demonstrated by Fresnel)

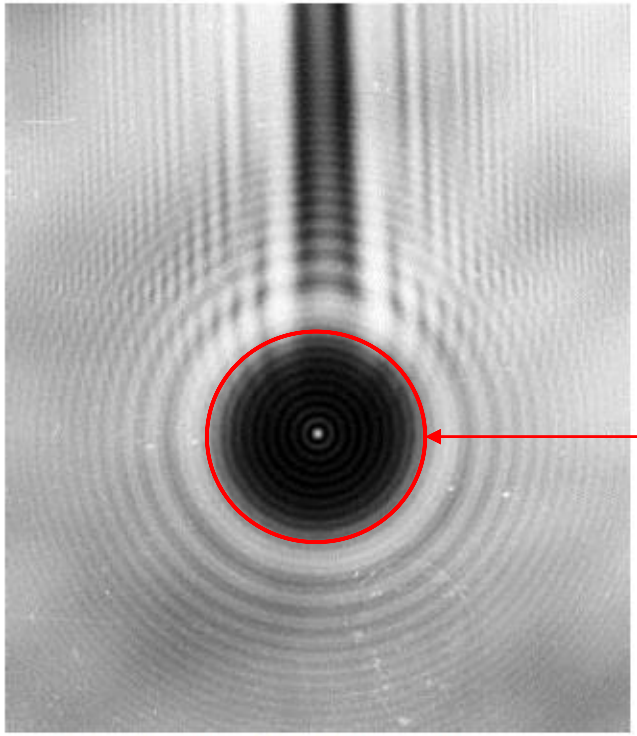

Geometrical umbra

Credit: Minerva.union.edu

Diffraction by an external occulter

- The **sharp-edged** occulting disk

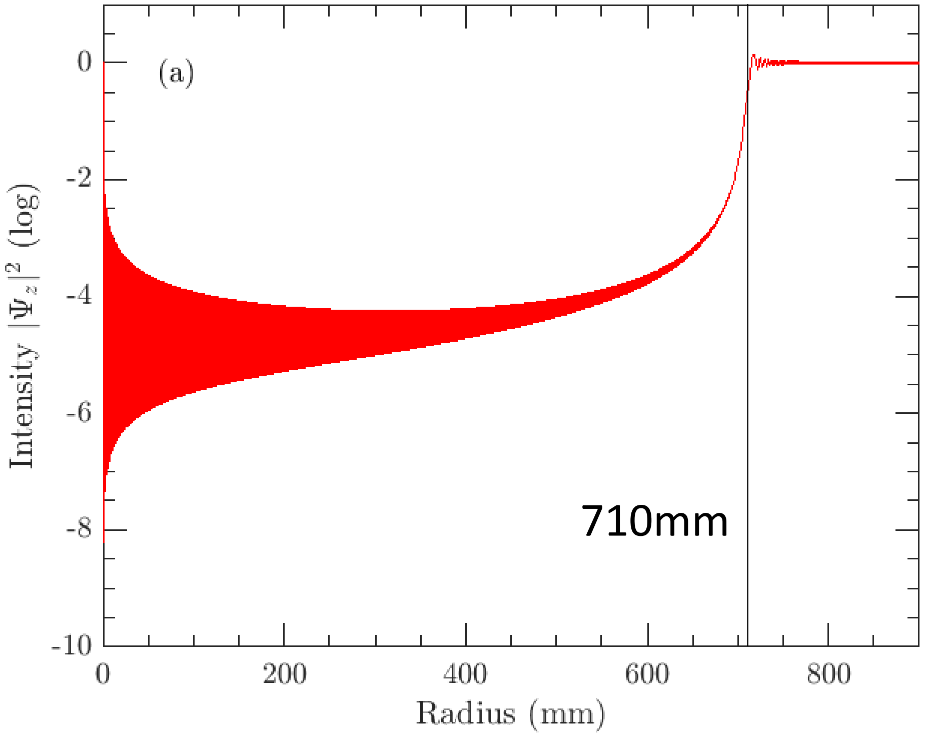

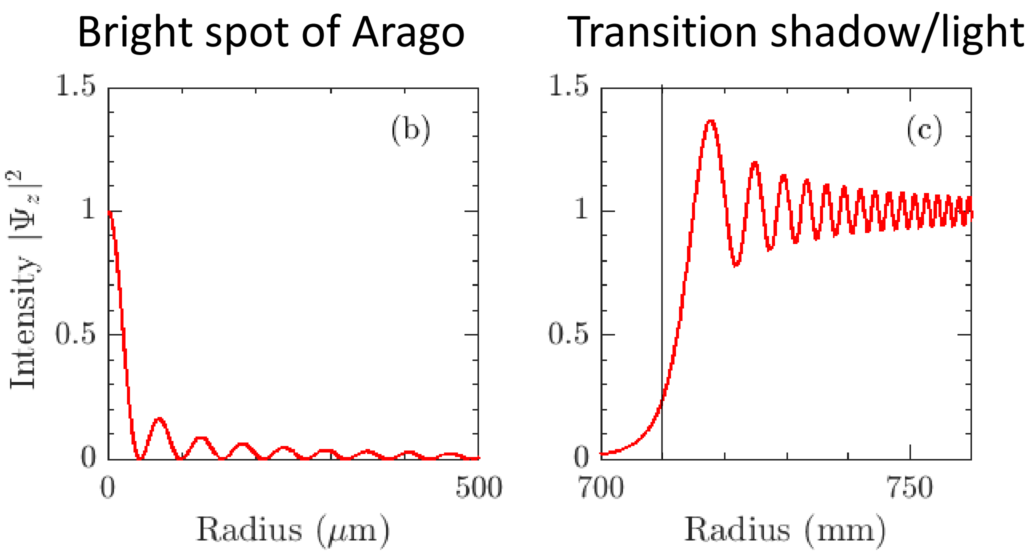

Diffraction by an external occulter

- The **apodized** occulting disk

Variable radial transmission

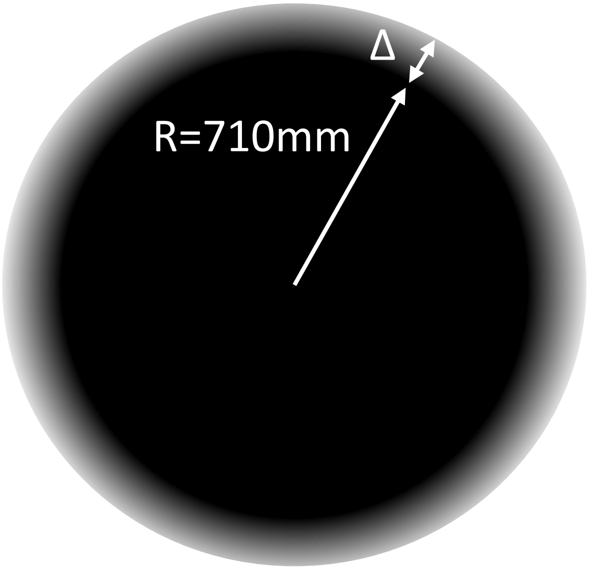

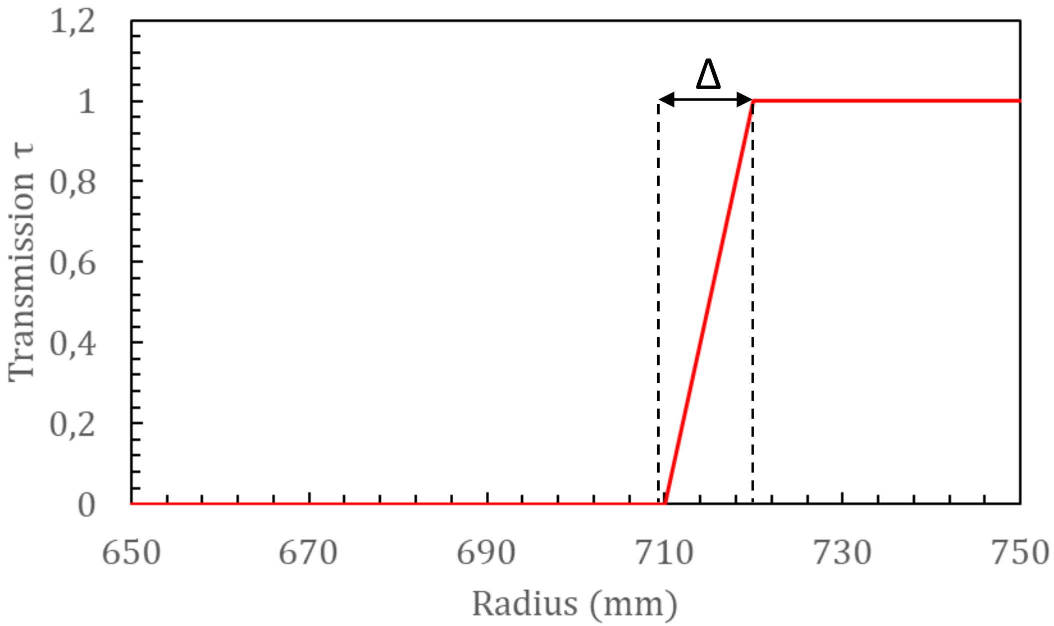

Diffraction by an external occulter

- The **apodized** occulting disk

$\Delta = 20mm$

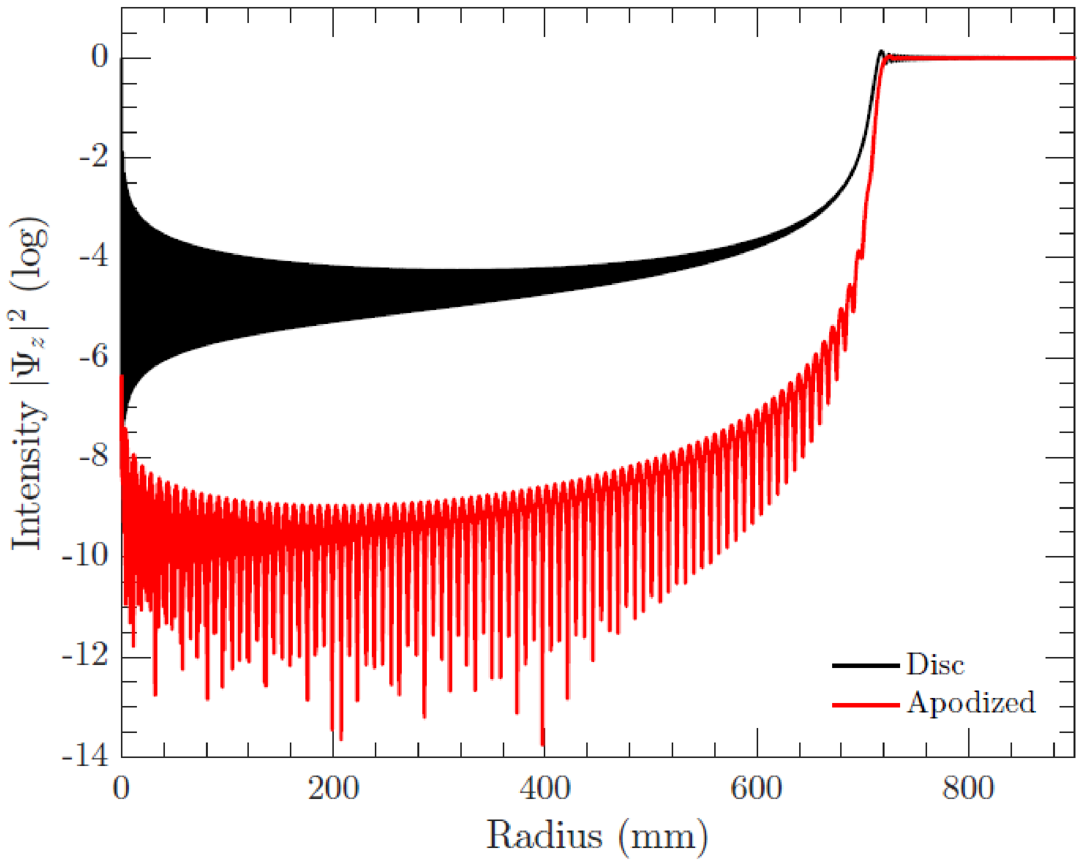

Diffraction by an external occulter

- The **serrated** (or petalized) occulter

  In **stellar coronagraphy**, the reasoning starts from the ideal apodized occulter

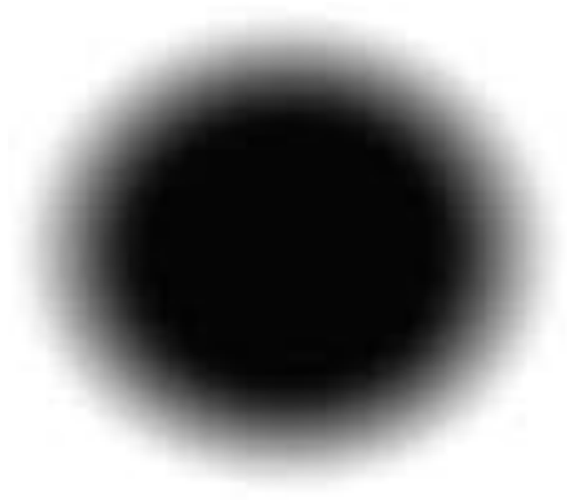

$$\tau_{apod}(r) = \int \tau_{petal}(r,\theta)d\theta$$

Cady, 2006
Vanderbei et al., 2007

The petalized occulter is the **discrete substitute**

Diffraction by an external occulter

- The **serrated** (or saw-toothed) occulter

  In **solar coronagraphy**, the reasonning is well different!

  The diffraction occurs perpendicularly to the edge
  A toothed disc rejects the light outside the central region

  Boivin (1978) predicted the radius of the dark inner region of the diffraction pattern based on geometrical considerations

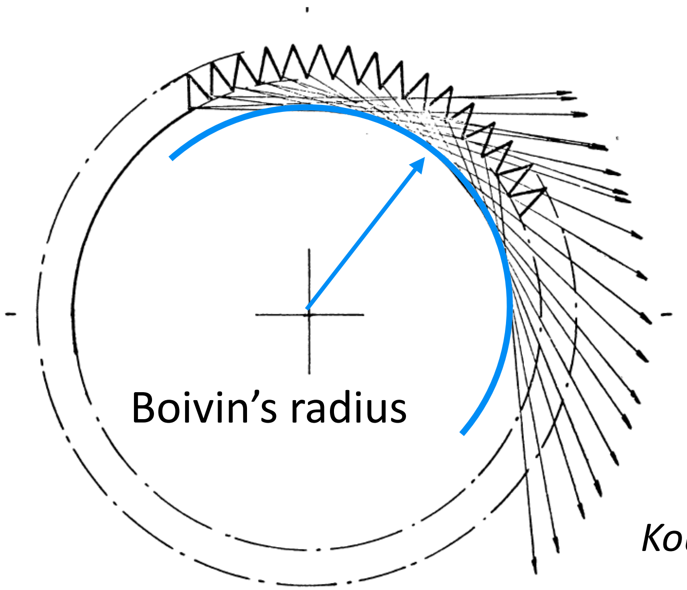

Koutchmy, 1988

Diffraction by an external occulter

- The **serrated** (or saw-toothed) occulter

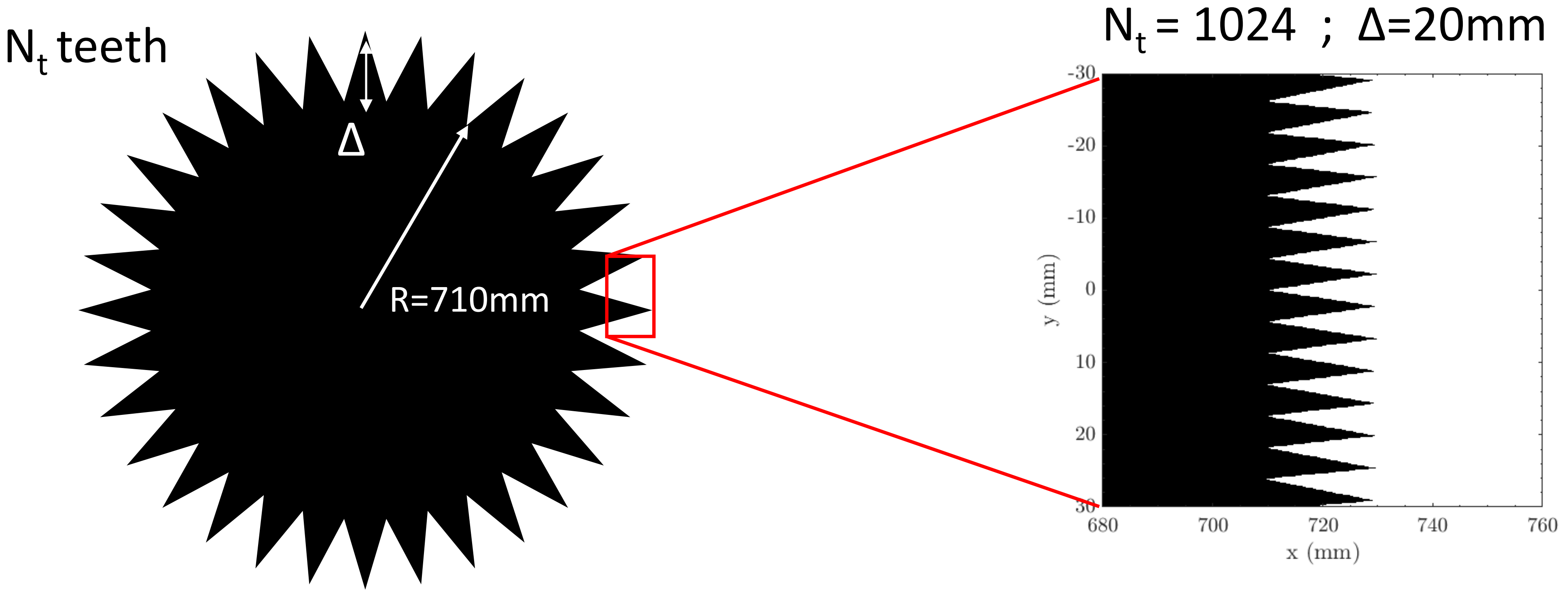

Diffraction by an external occulter

- The **serrated** (or saw-toothed) occulter

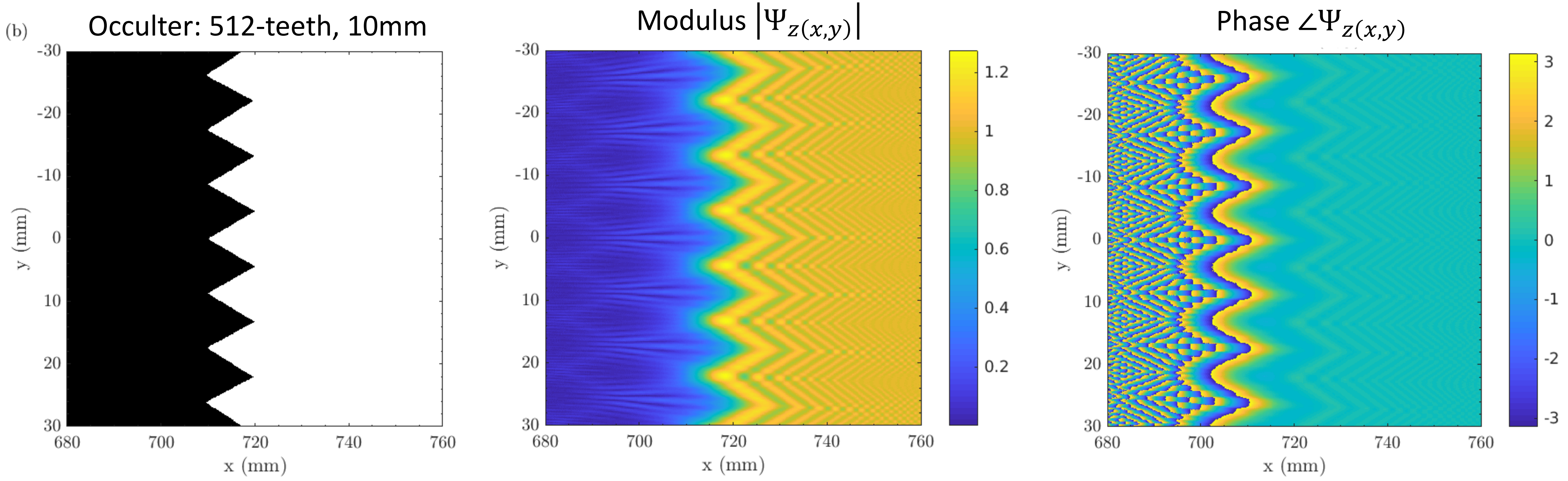

Diffraction by an external occulter

- The **serrated** (or saw-toothed) occulter

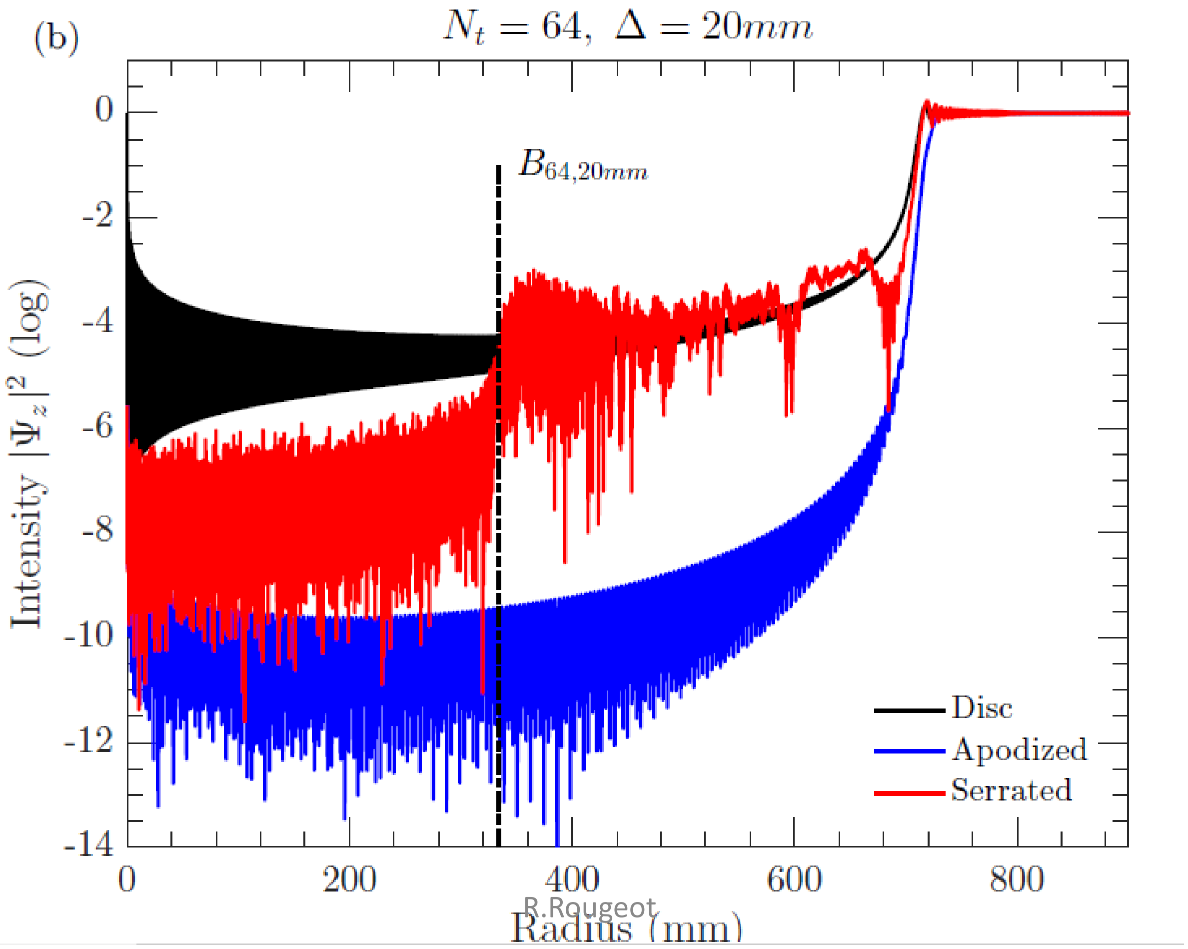

Diffraction by an external occulter

- The **serrated** (or saw-toothed) occulter

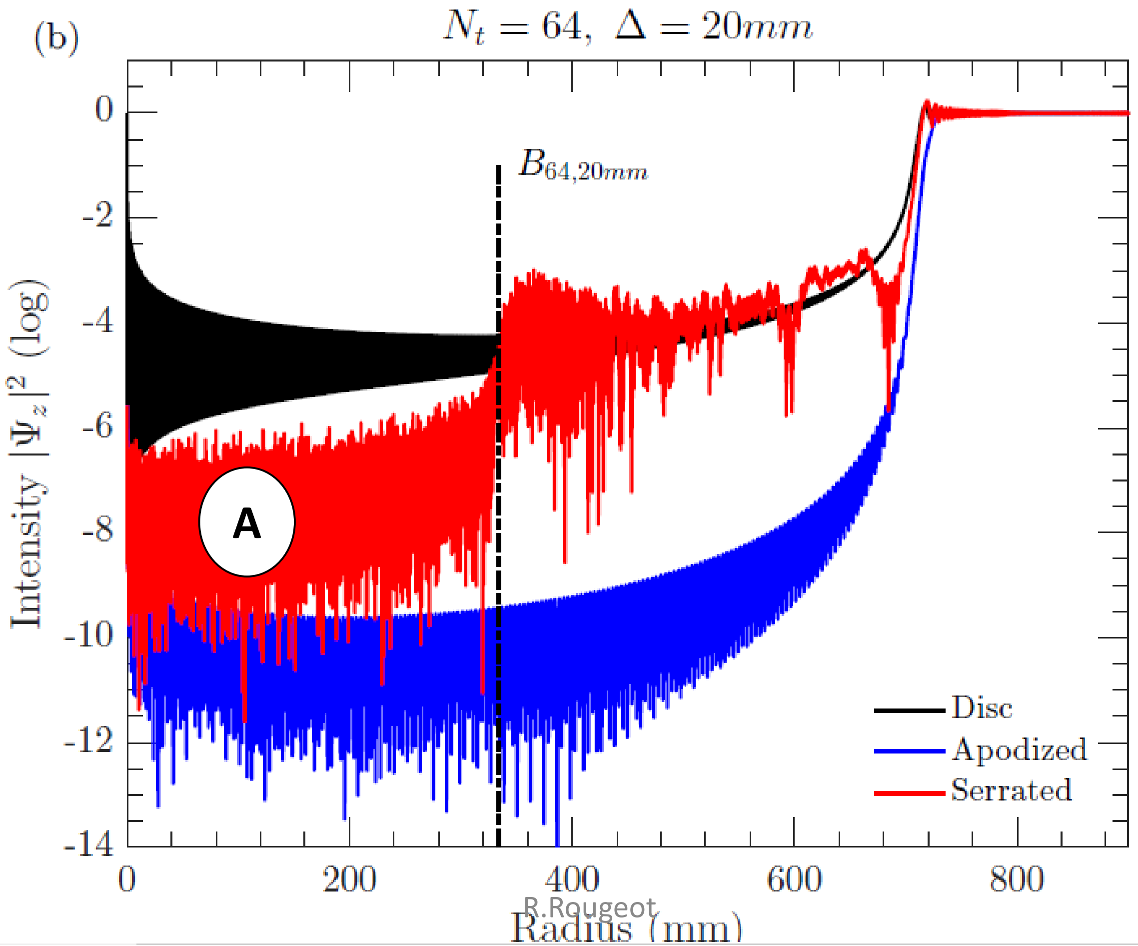

A Dark inner region

Diffraction by an external occulter

- The **serrated** (or saw-toothed) occulter

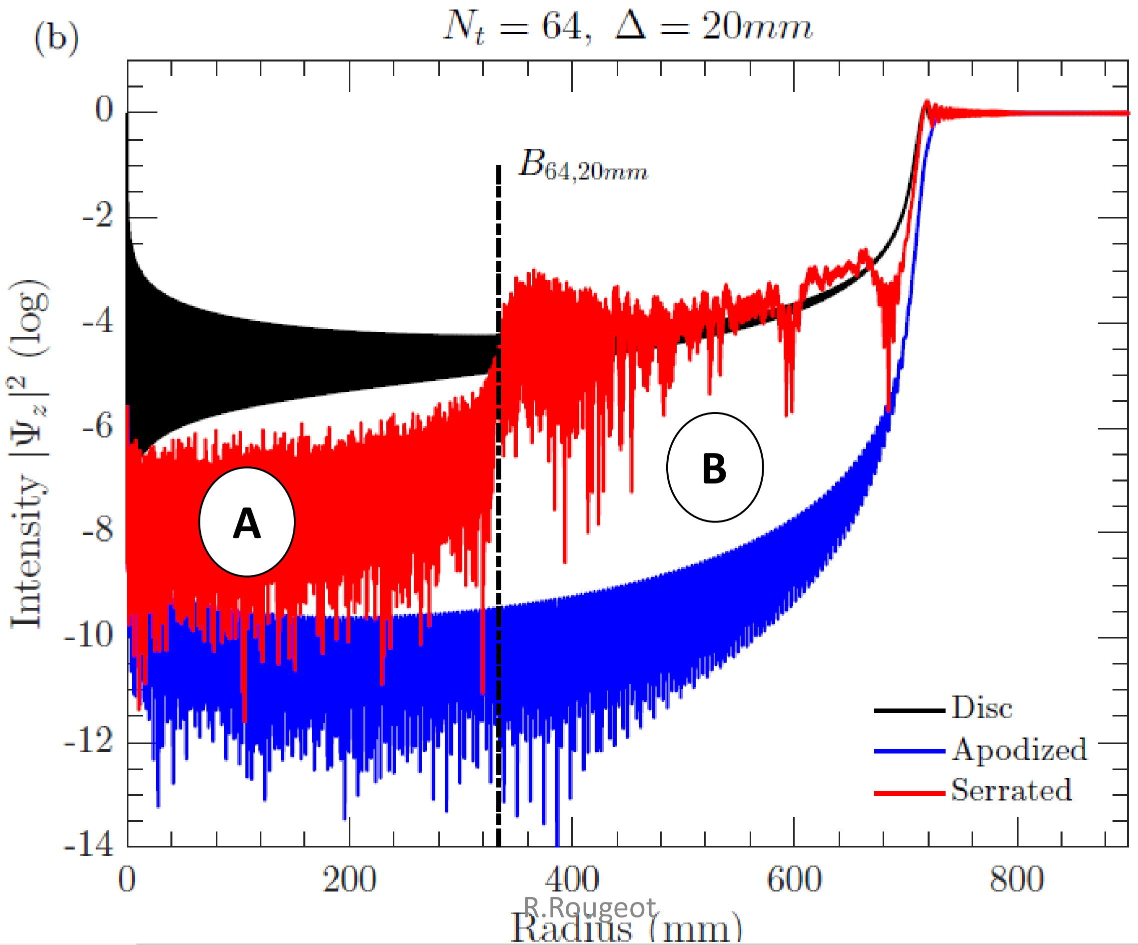

A Dark inner region

B Intermediate region

Diffraction by an external occulter

- The **serrated** (or saw-toothed) occulter

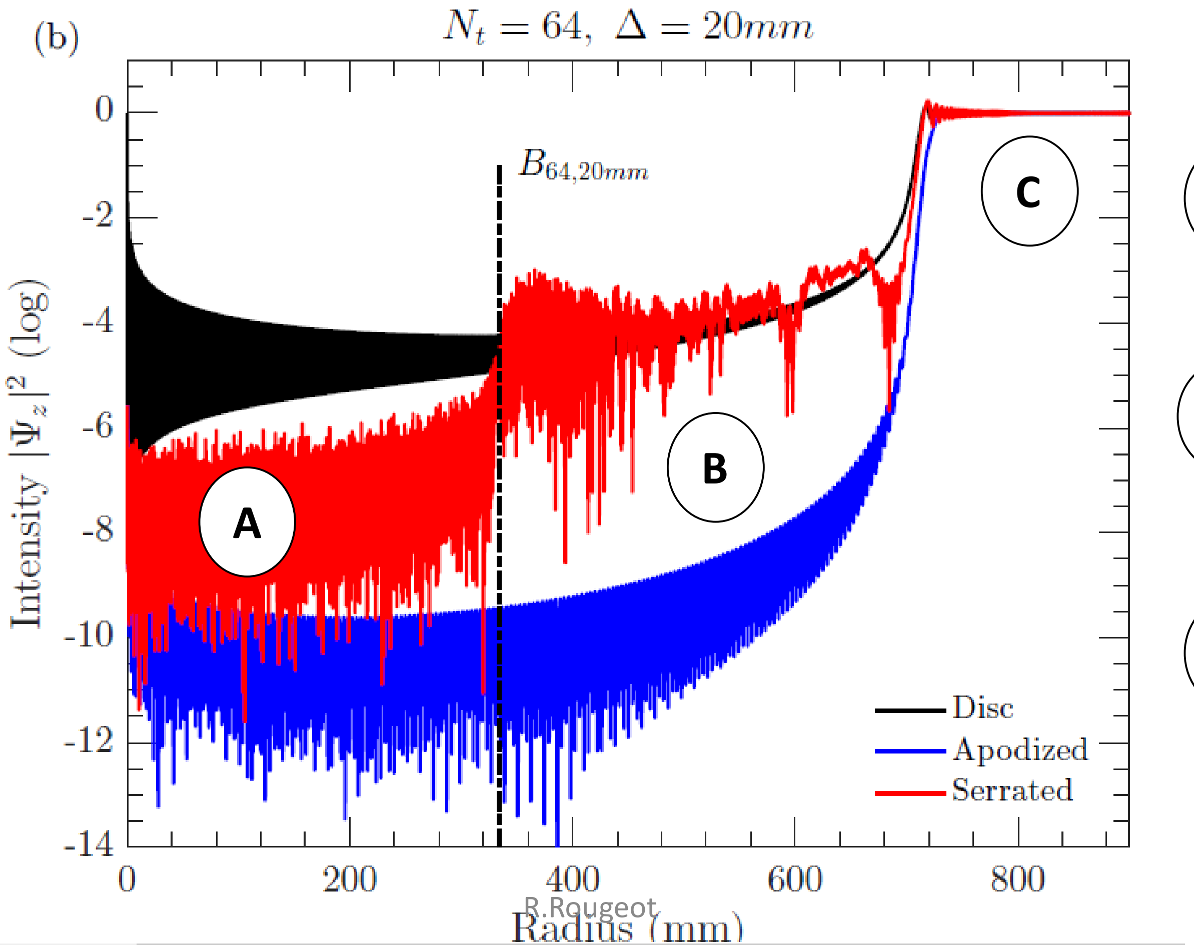

A Dark inner region

B Intermediate region

C Fully illuminated region

Diffraction by an external occulter

- We numerically verified the geometrial predictions of Boivin (1978)

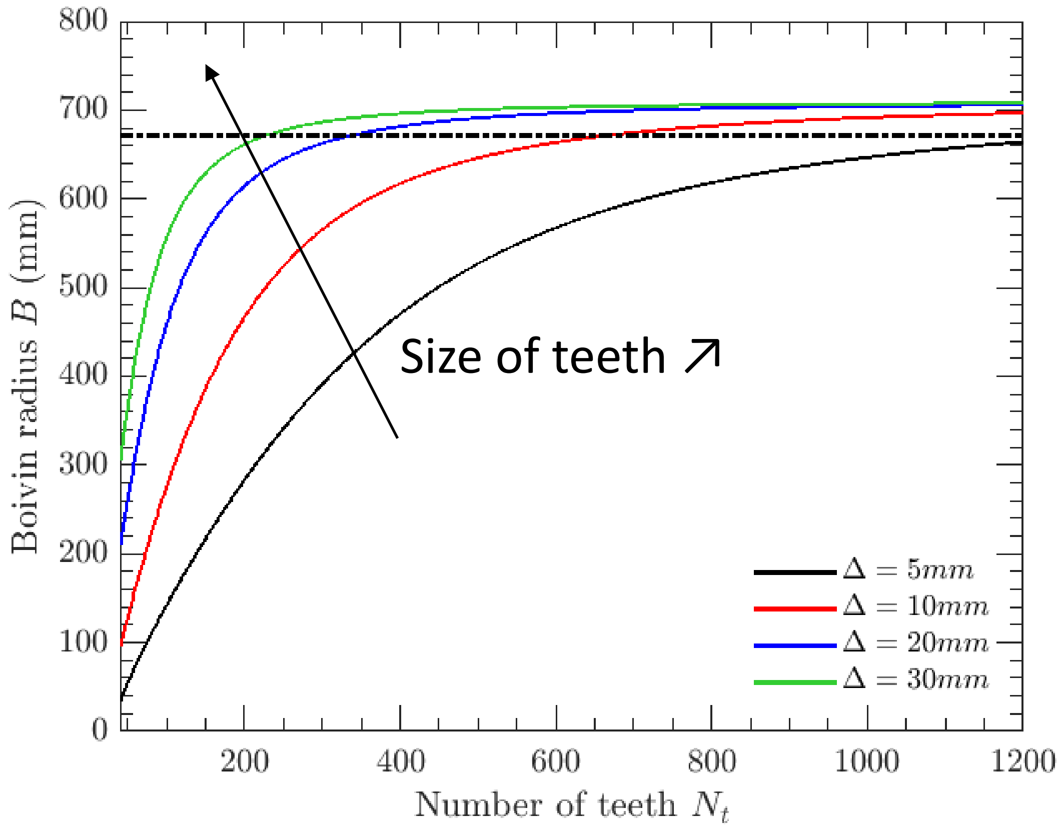

Rougeot & Aime, 2018

Diffraction by an external occulter

- The **serrated** (or saw-toothed) occulter

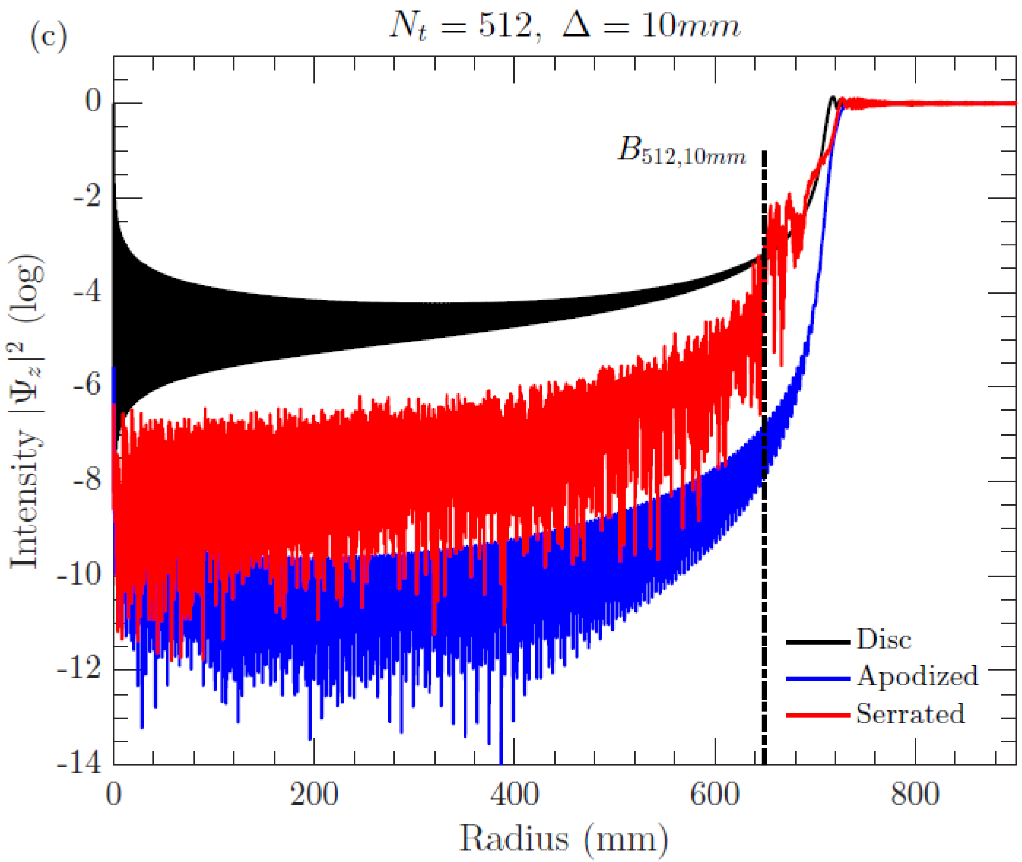

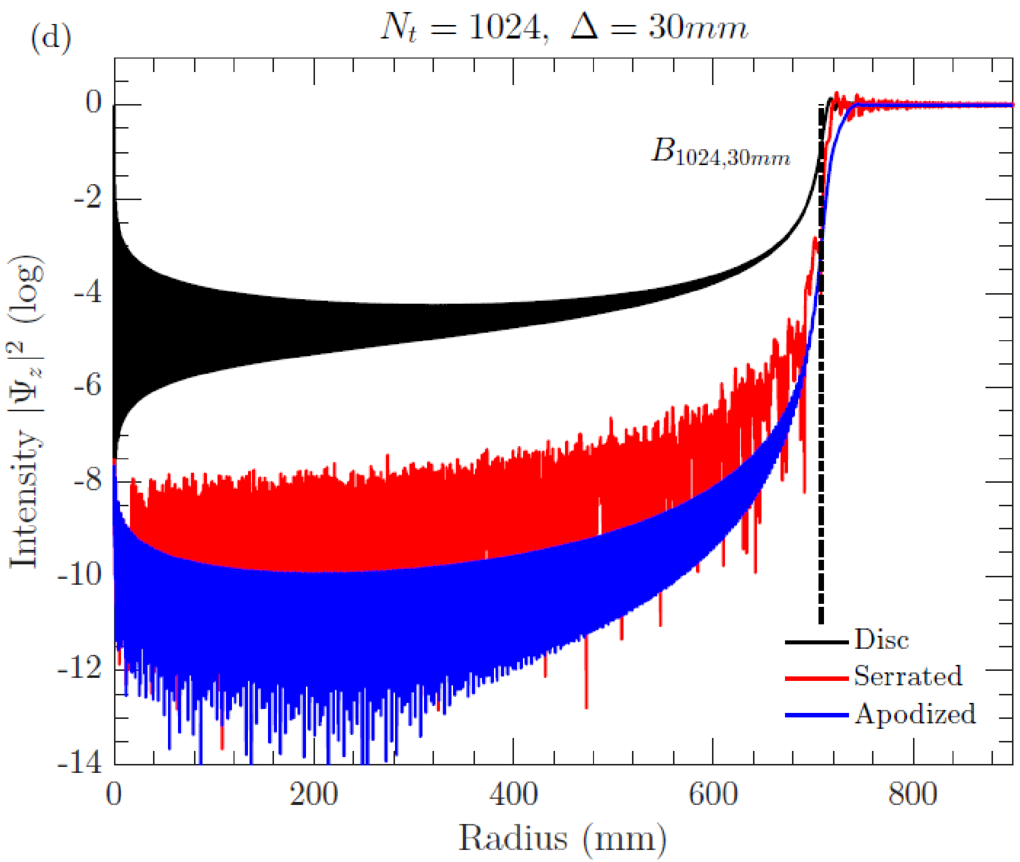

Penumbra profile

Penumbra profiles

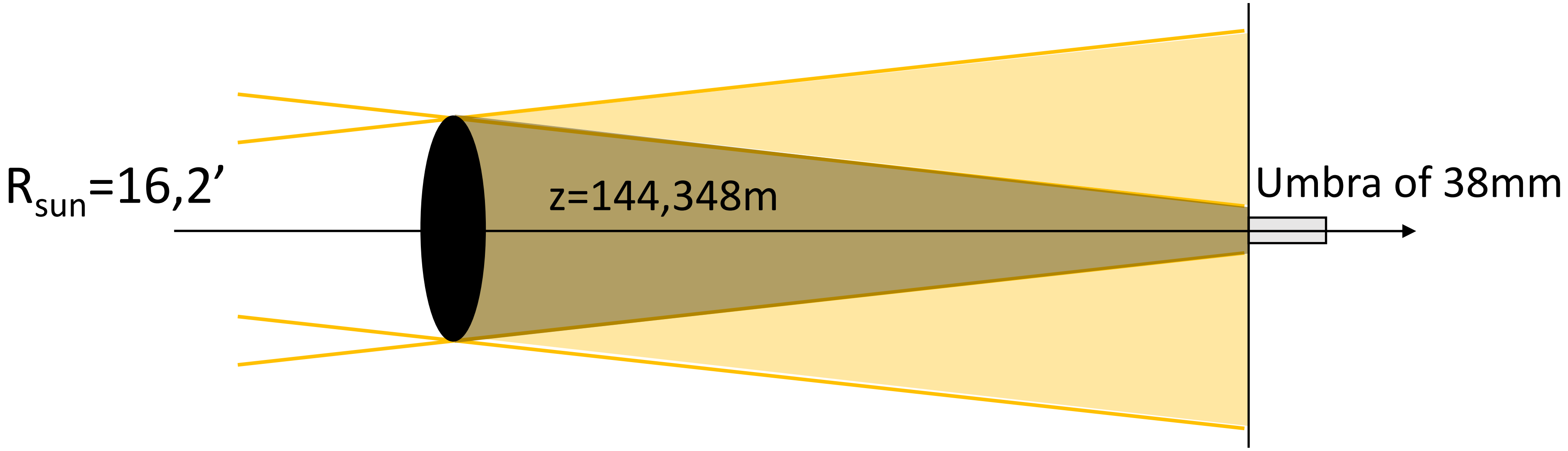

- **Convolution** of the diffraction pattern $|\Psi_z(x, y)|^2$ with the solar disk
  Centre-to-limb darkening function

Penumbra profiles

- The **sharp-edged** occulting disk

$I_z(r = 0) \approx 10^{-4} \mathrm{I}_{\mathrm{sun}}$

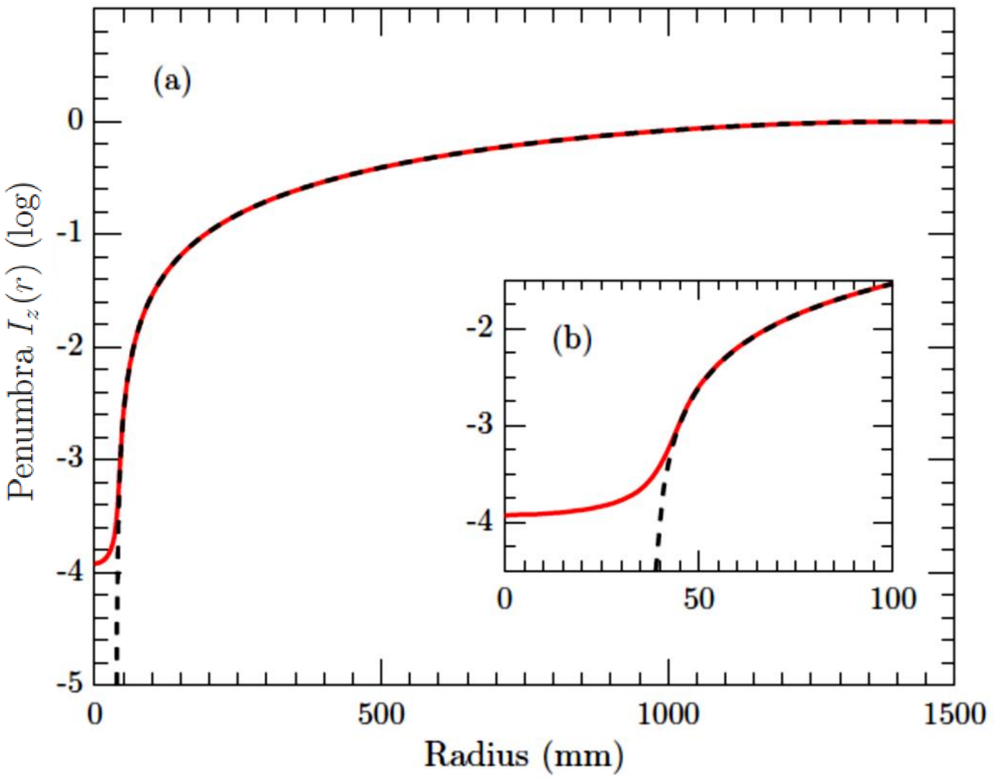

Diffraction

Purely geometrical

Penumbra profiles

- The **serrated** (or saw-toothed) occulter

Δ=20mm

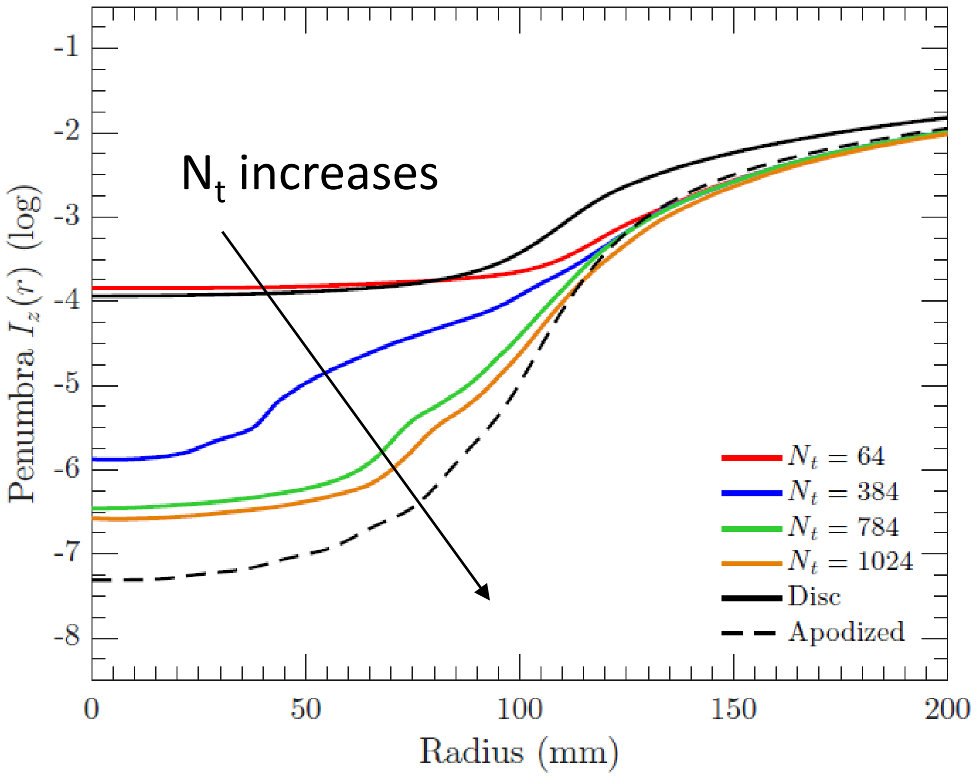

N_t=464

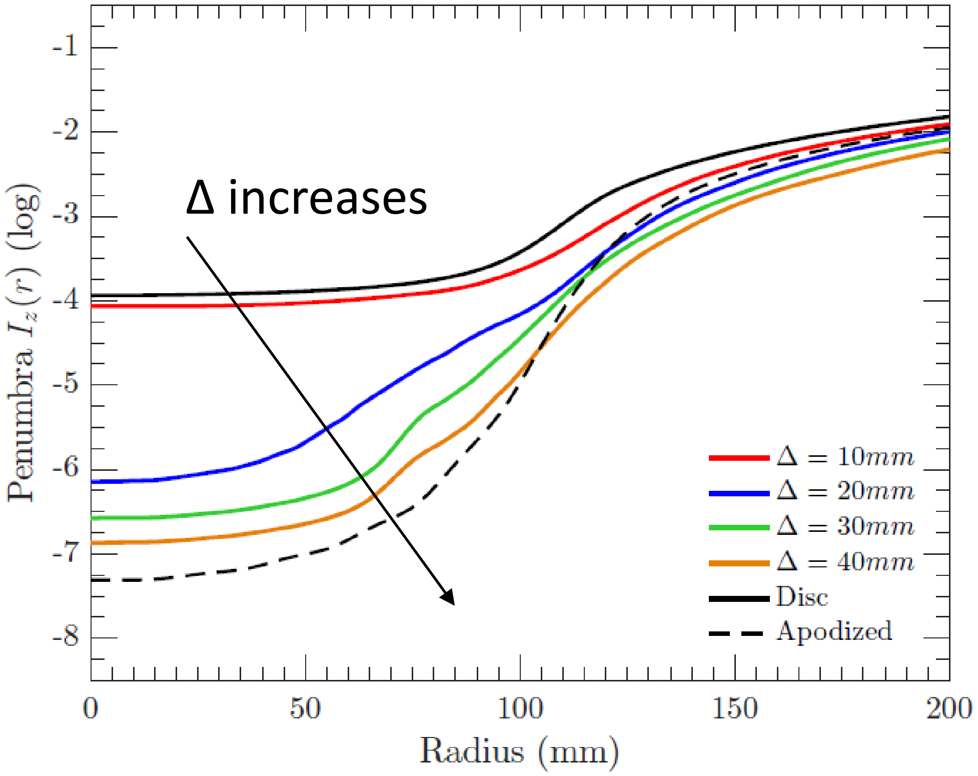

Penumbra profiles

- The **serrated** (or saw-toothed) occulter

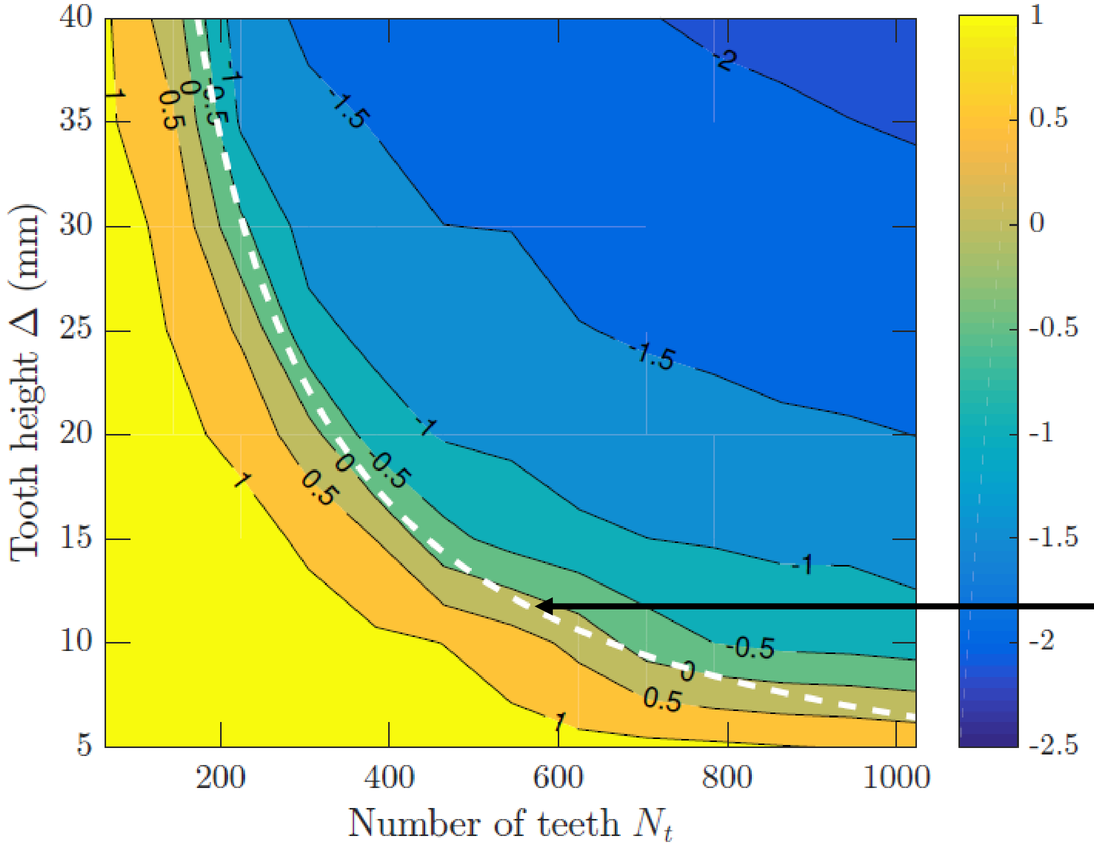

Integrated illumination over the pupil, normalized to the sharp-edged disk cas

$$\frac{\iint_{pupil} I_{serrated}\, ds}{\iint_{pupil} I_{sharp}\, ds}$$

Boivin radius$(N_t, \Delta) > r_{sun}$ =671mm

Conclusion

Conclusion

- Model of diffraction for external occulters in solar coronagraphy
  - Limits of Fresnel diffraction integrals using 2D FFT
  - Maggi-Rubinowicz representation

- Assessement of the theoretical performance of serrated occulters

- References

  - Aime C. 2013, A&A, 558, A138
  - Rougeot R., Flamary R., Galano D., Aime C. 2017, A&A, 599, A2
  - Rougeot R., Aime C. 2018, A&A, 612, A80

Other works

- Propagation of the diffracted wavefronts inside the Lyot-style coronagraph
  - end-to-end performance in straylight rejection
  - impacts of the size of the internal occulter and the Lyot stop
  - PSF in the vignetting zone

- On-going/future works:
  - optical aberrations of the optics
  - effects of surface roughness scattering

Questions?

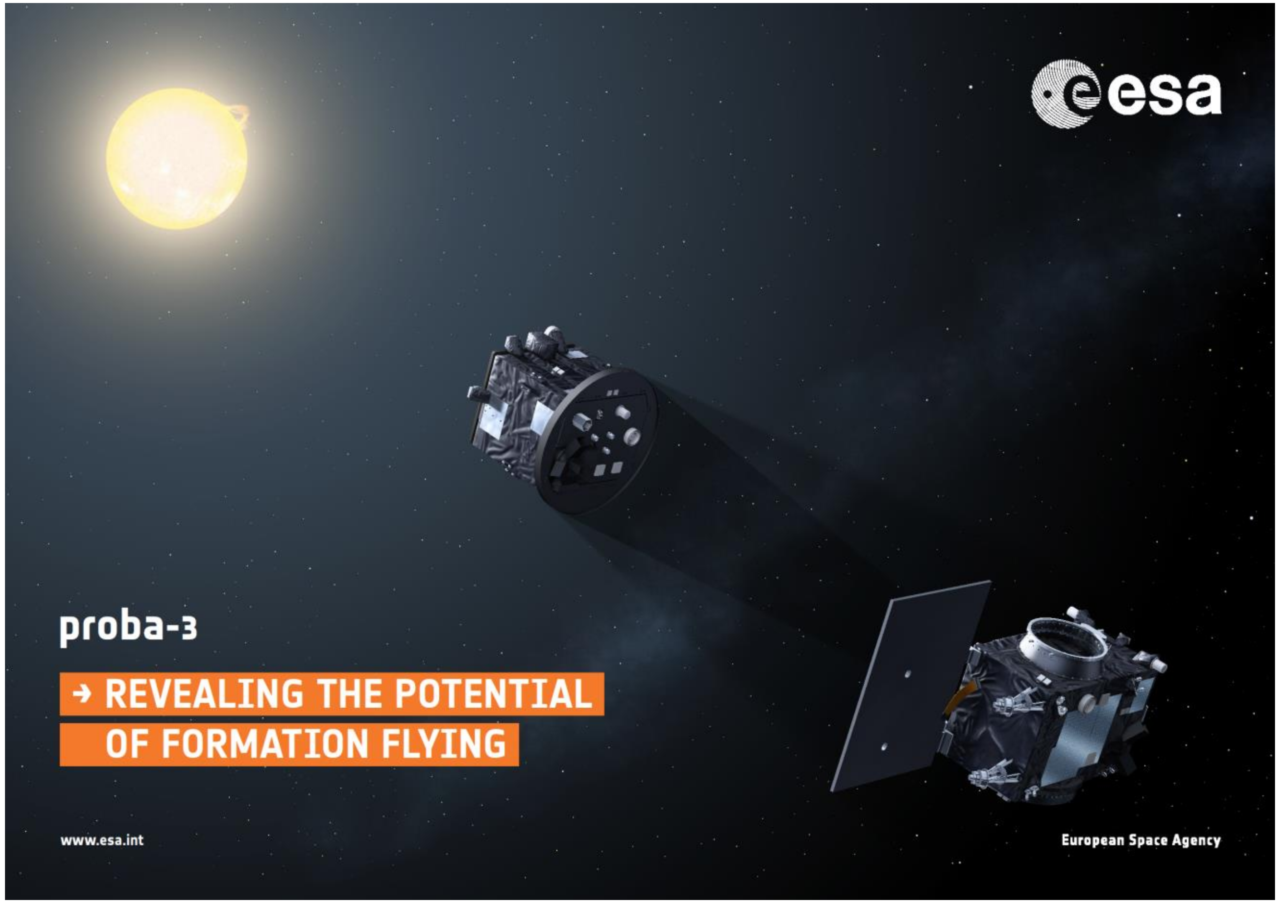

Thank you for your attention!

Propagation inside the coronagraph

Propagation inside the coronagraph

- The hybrid externally occulted Lyot solar coronagraph ASPIICS

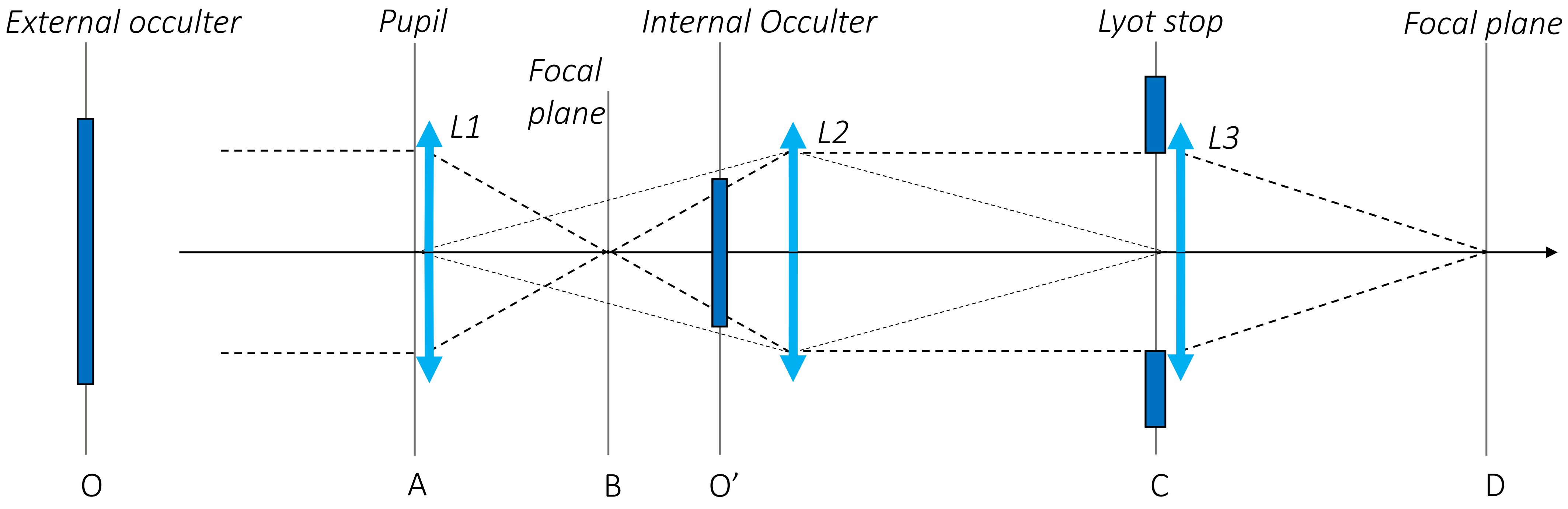

Propagation inside the coronagraph

- **Propagation of the diffracted wavefront** from one plane to the next one:
  - Fourier optics formalism
  - ideal optics
  - perfect axis-symetric geometry

- Numerical implementation: successive FFT with arrays of large size

- Objective:
  - estimate the level and spatial distribution of the residual diffracted sunlight
  - address the rejection performance of the coronagraph

Propagation inside the coronagraph

- Intensity in plane O', where the internal occulter is set

Without external occulter

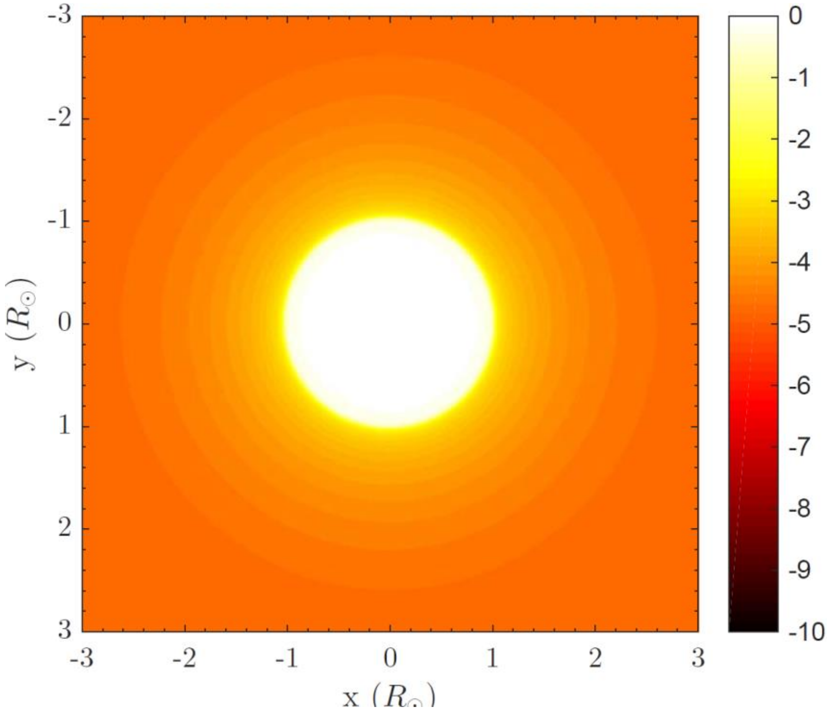

With external occulter

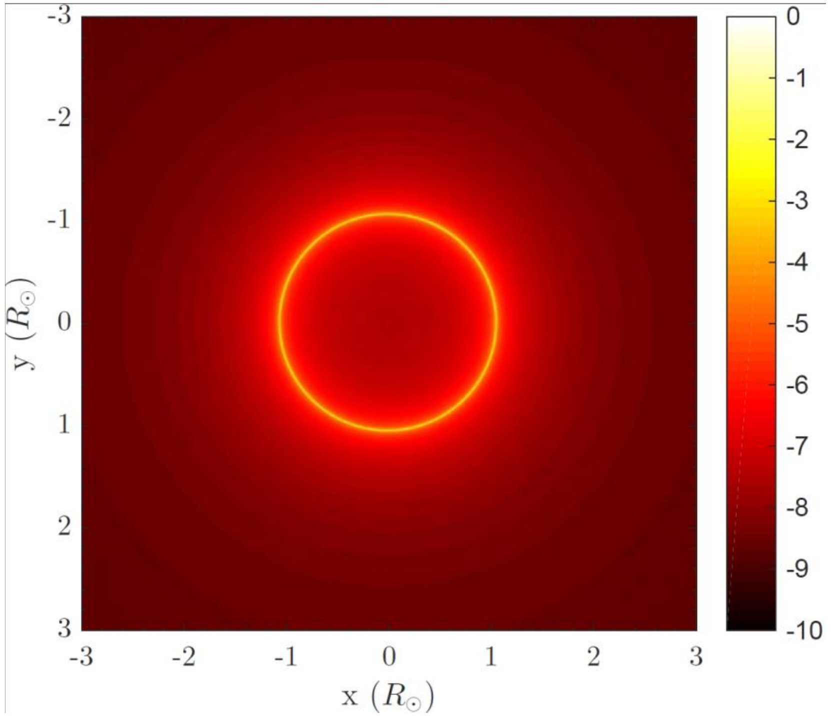

Propagation inside the coronagraph

- Intensity in plane O', where the internal occulter is set

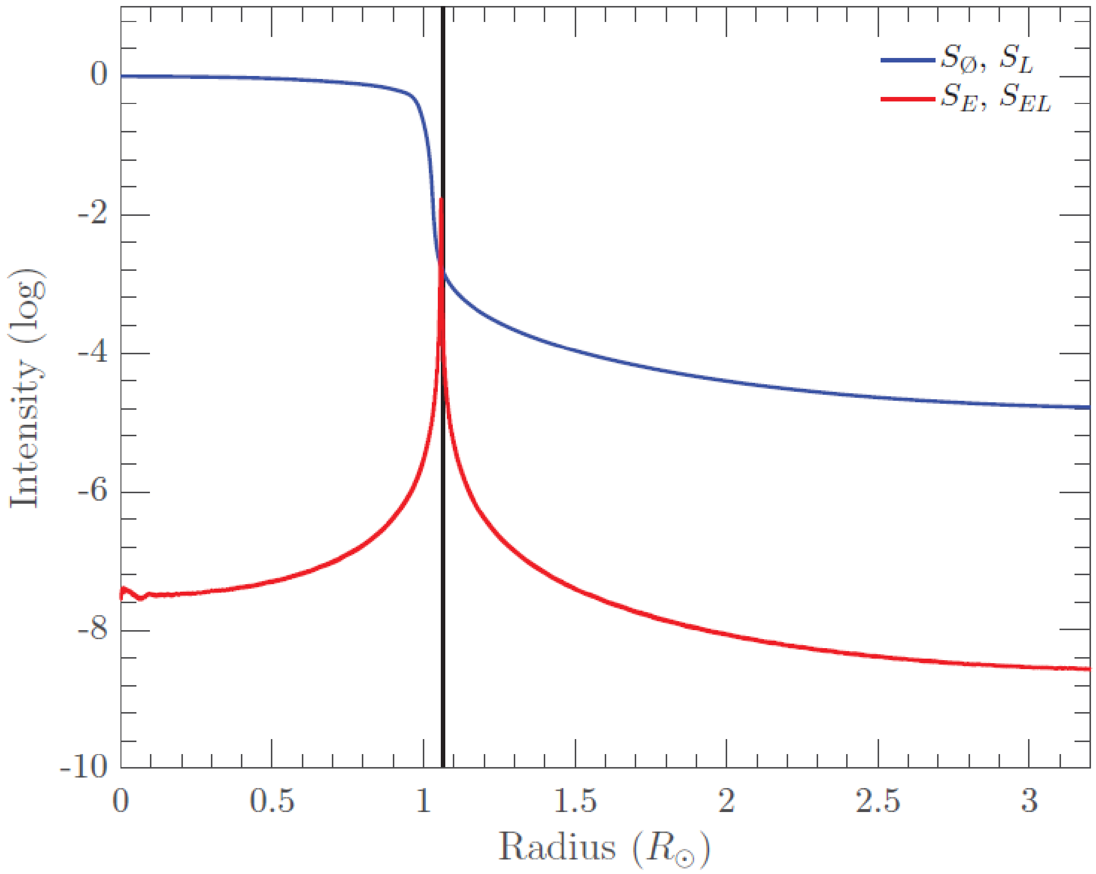

With external occulter

Without external occulter
Solar disk image (out-of-focused)

Rougeot et al., 2017

Propagation inside the coronagraph

- Intensity in plane O’, where the internal occulter is set

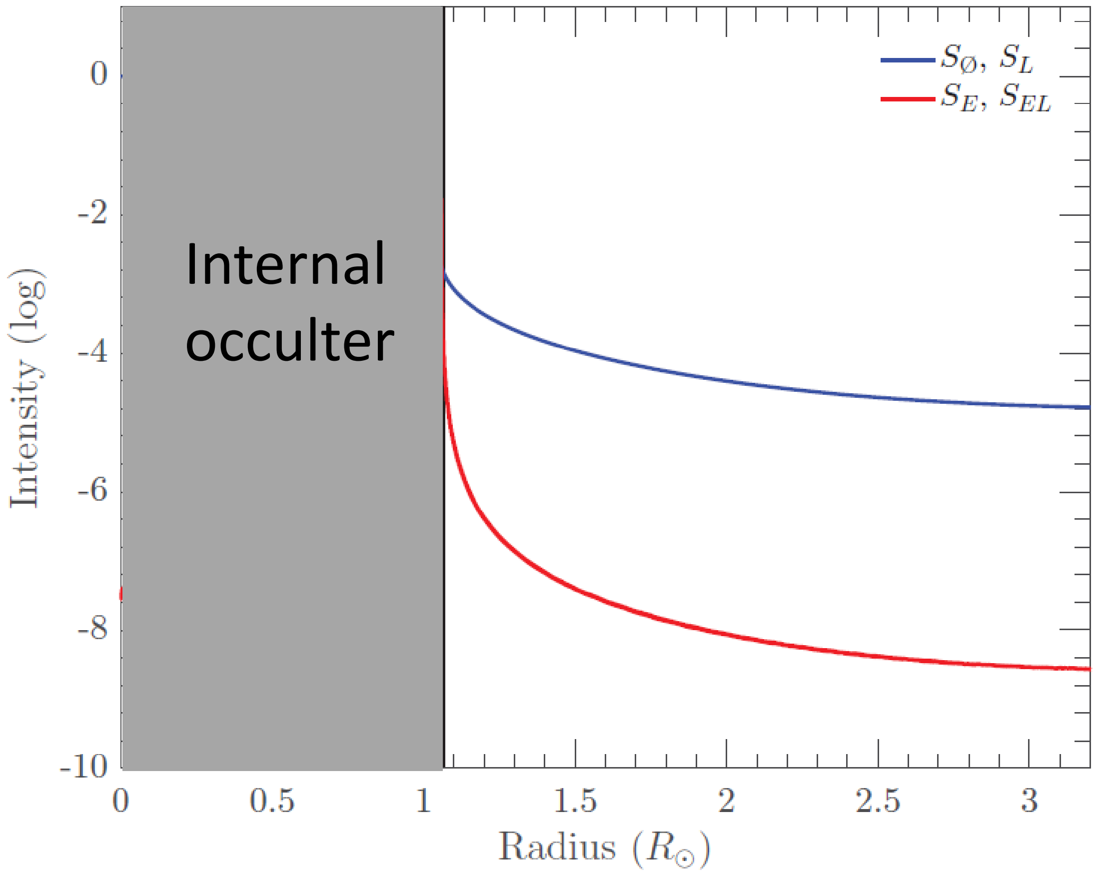

With external occulter

Without external occulter
Solar disk image (out-of-focused)

Propagation inside the coronagraph

- Intensity in plane C, where the Lyot stop is set

Without external occulter

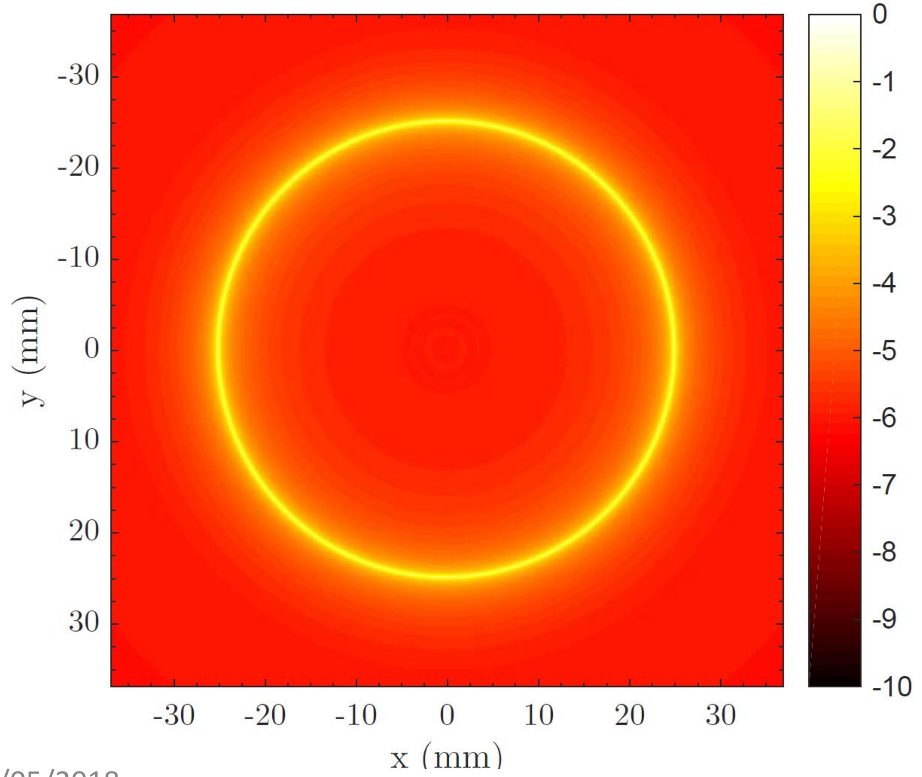

With external occulter

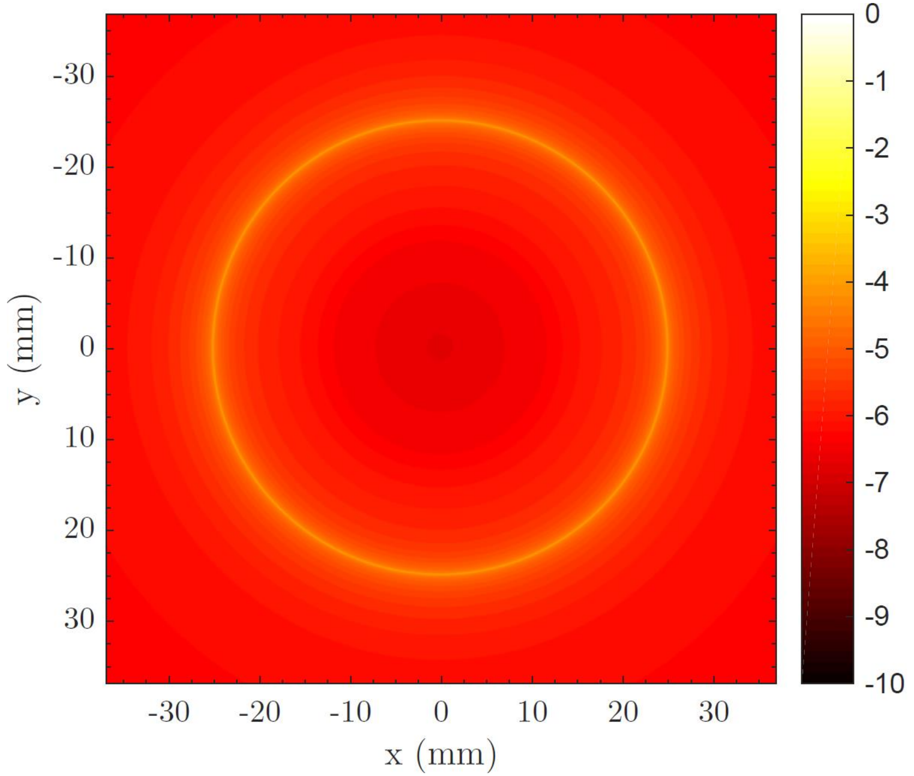

Propagation inside the coronagraph

- Intensity in plane C, where the Lyot stop is set

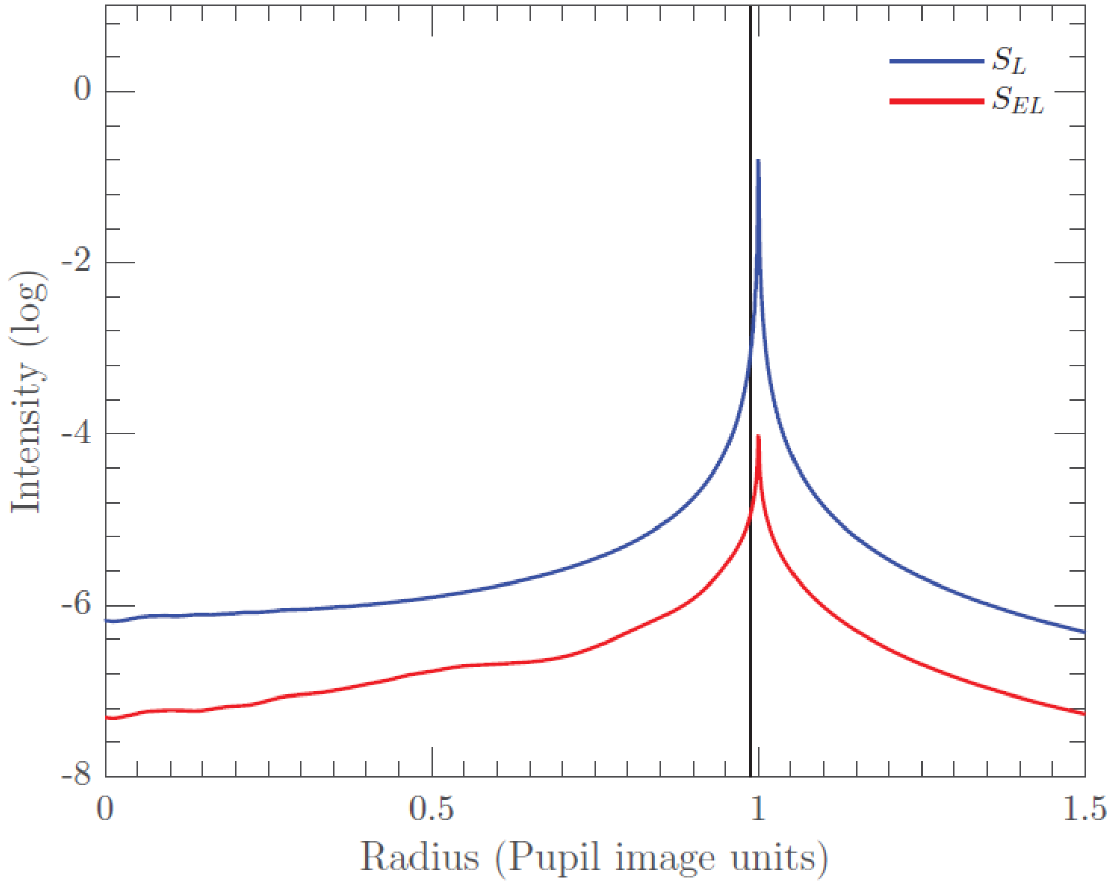

With external occulter

Without external occulter (Lyot coronagraph)

Propagation inside the coronagraph

- Intensity in plane C, where the Lyot stop is set

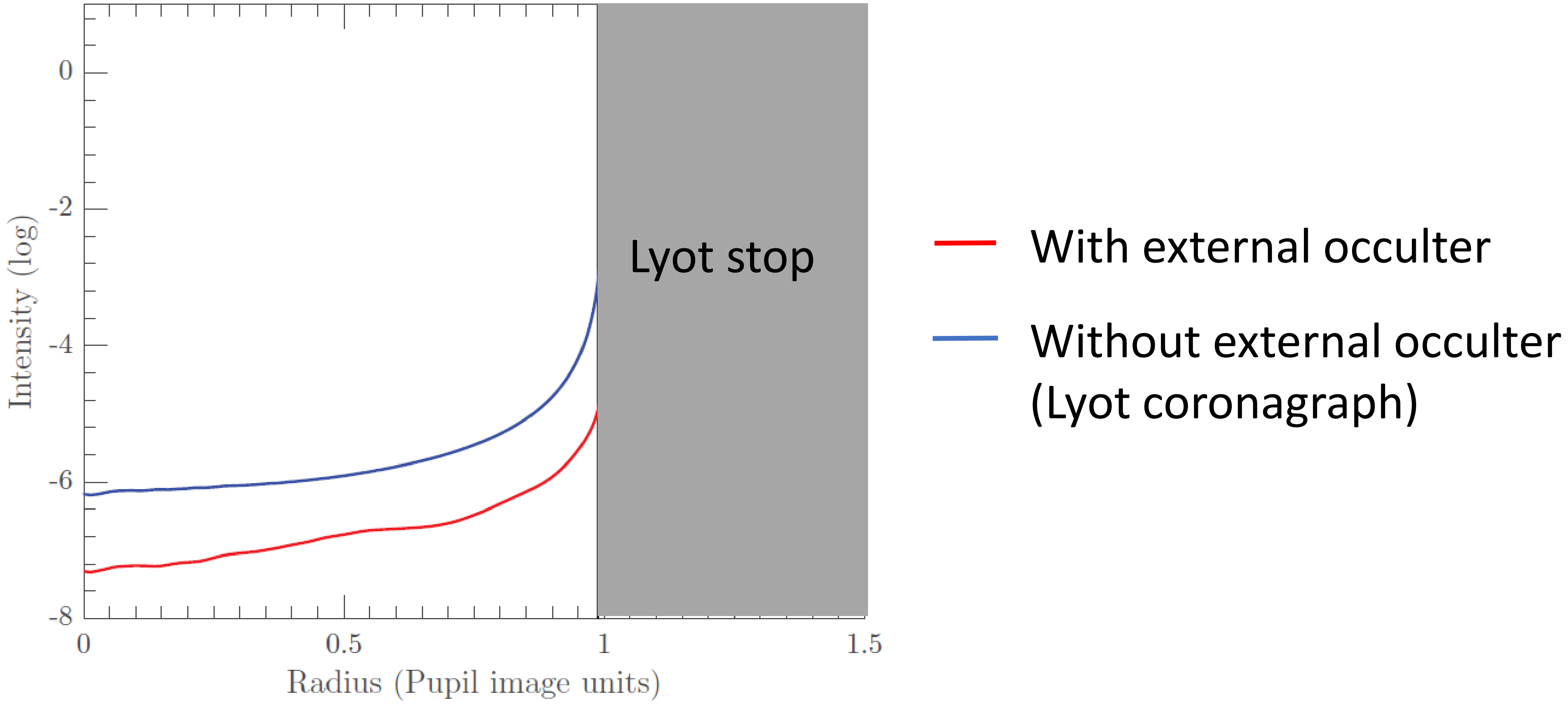

Propagation inside the coronagraph

- Intensity in plane D, final focal plane with the detector

With external occulter

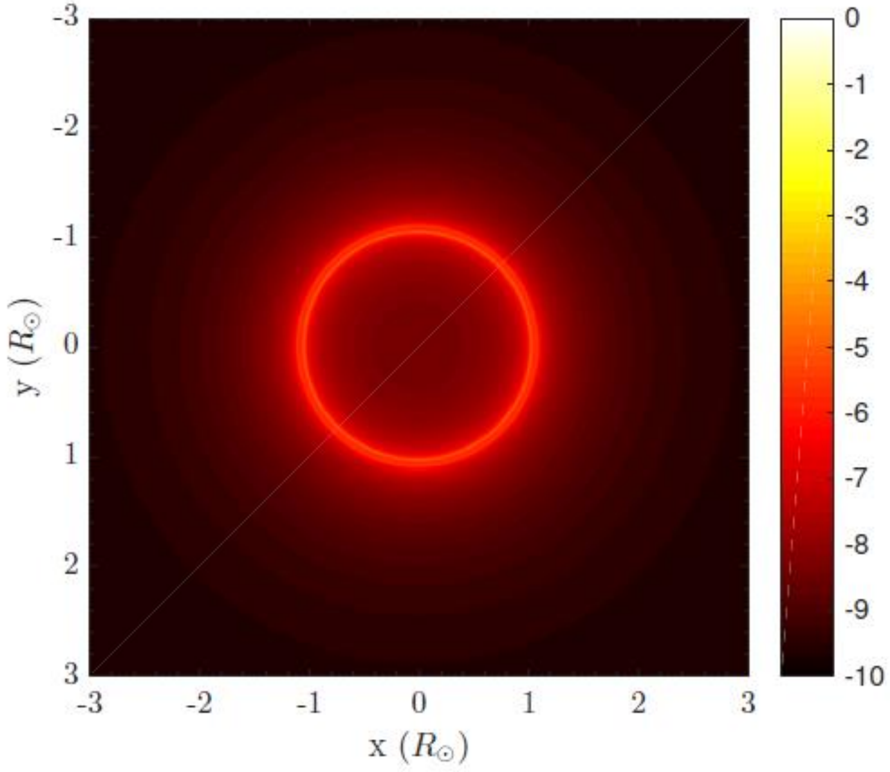

Propagation inside the coronagraph

- Intensity in plane D, final focal plane with the detector

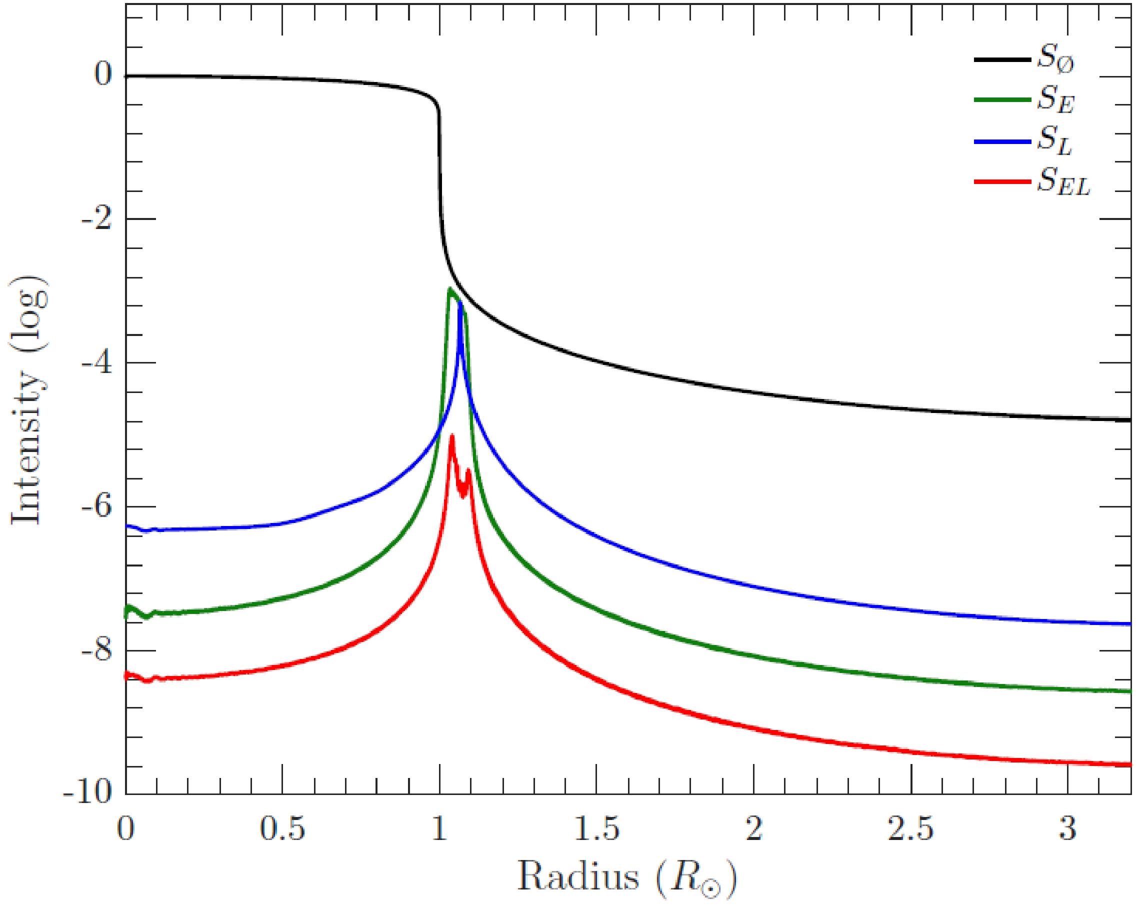

No occulter and stop
Solar disk image

Just the external occulter
No internal occulter
No Lyot stop

Without external occulter
(Lyot coronagraph)

With external/internal occulters and Lyot stop

Propagation inside the coronagraph

- Impact of **sizing** the internal occulter and the Lyot stop
  Intensity on plane D, the final focal plane

Fixed Lyot stop

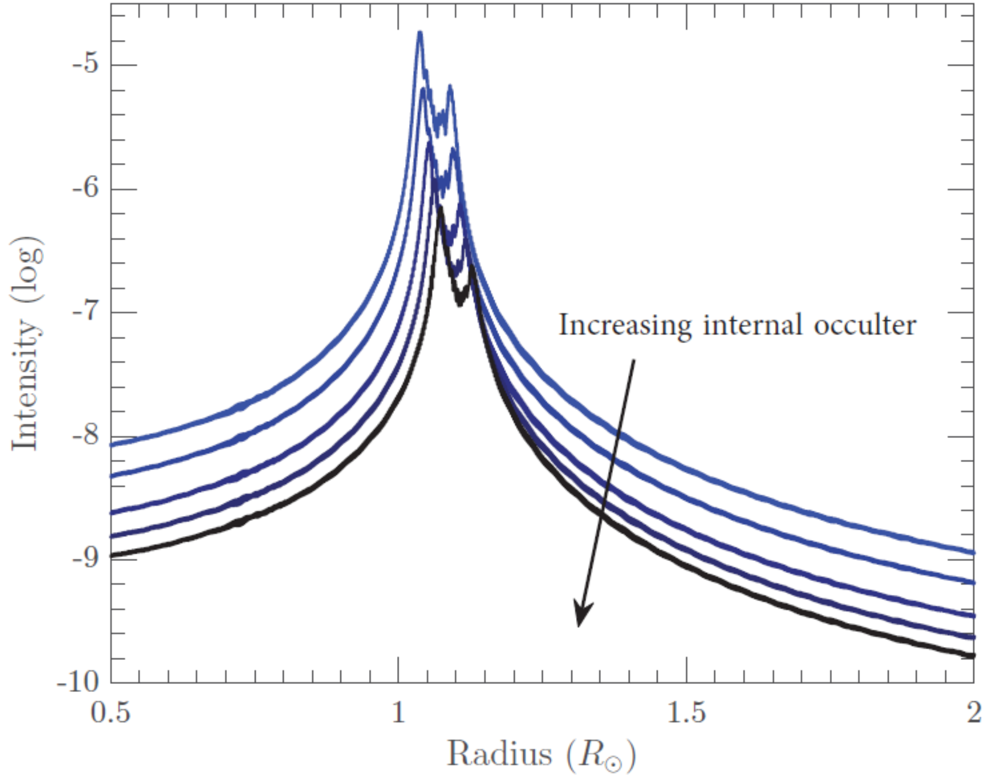

Fixed internal occulter

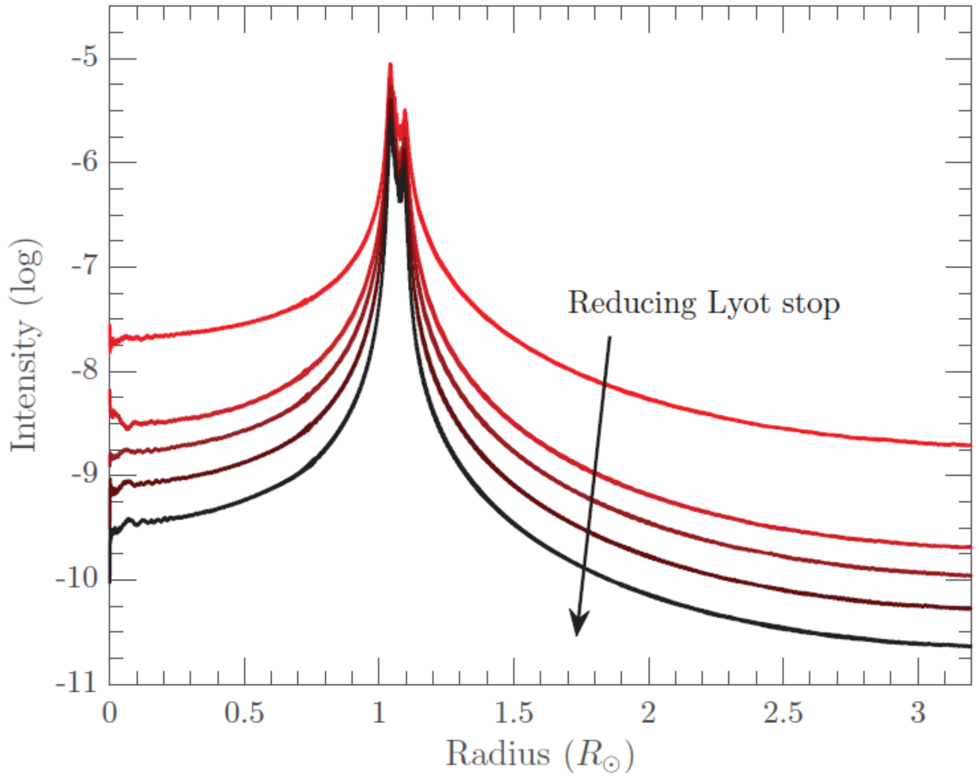

Propagation inside the coronagraph

- Impact of sizing the internal occulter and the Lyot stop

Residual diffracted sunlight @ $1.3R_{\odot}$

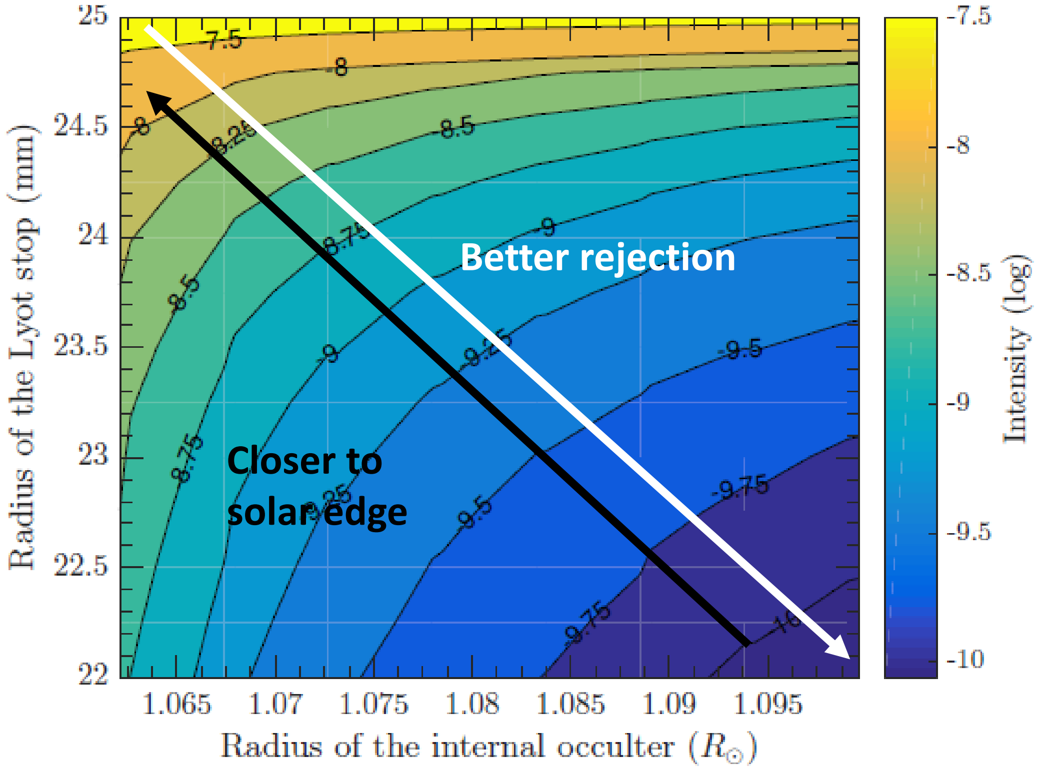

Propagation inside the coronagraph

- PSF in the **vignetted zone**

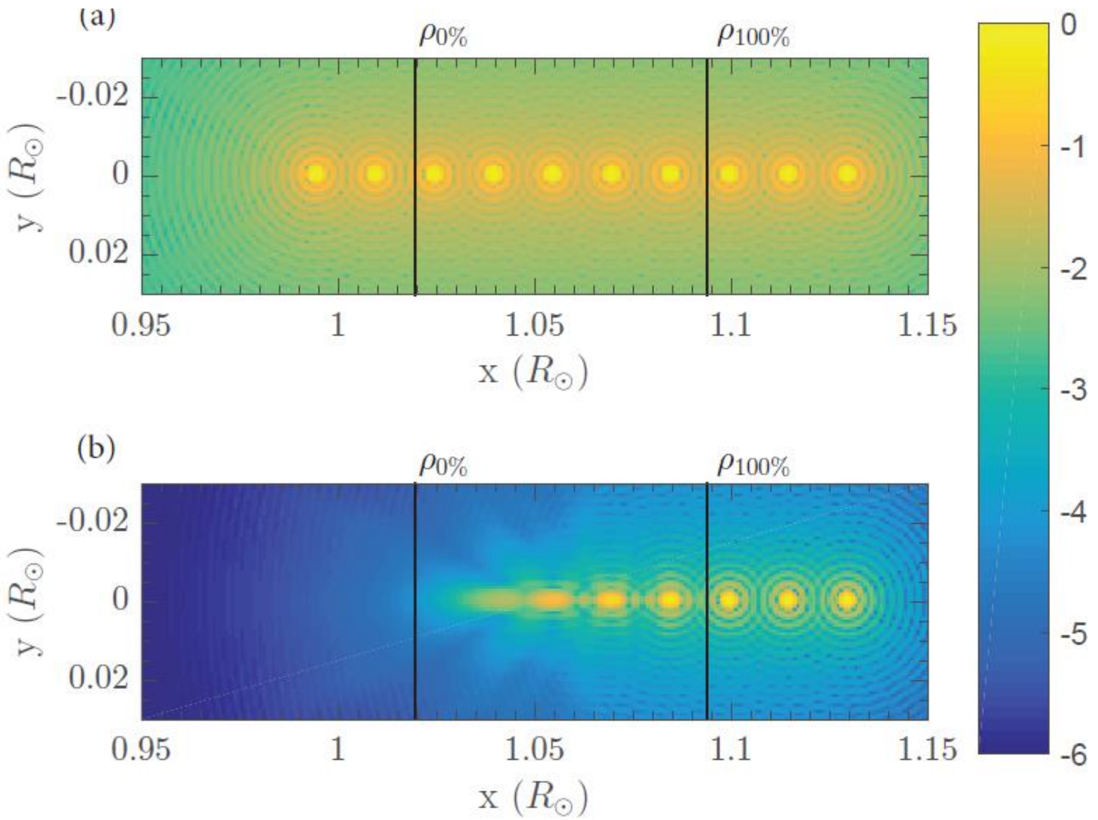

Annex on diffraction formulations

2D FFT technique

The **Fresnel filter** $\exp(i\pi\lambda z u^2)$ has its phase varying as u^2

At the edge of the array, $u_c = 1/2\sigma$

We impose that the (maximum) phase variation at the edge of the array is $<\pi$

$$\sigma > \sqrt{\frac{\lambda z}{K}}$$

Consequence: $\sigma \searrow \Longrightarrow K \nearrow$

2D FFT technique

Very sensitive to numerical sampling: impact of the size of the array

2D FFT computation

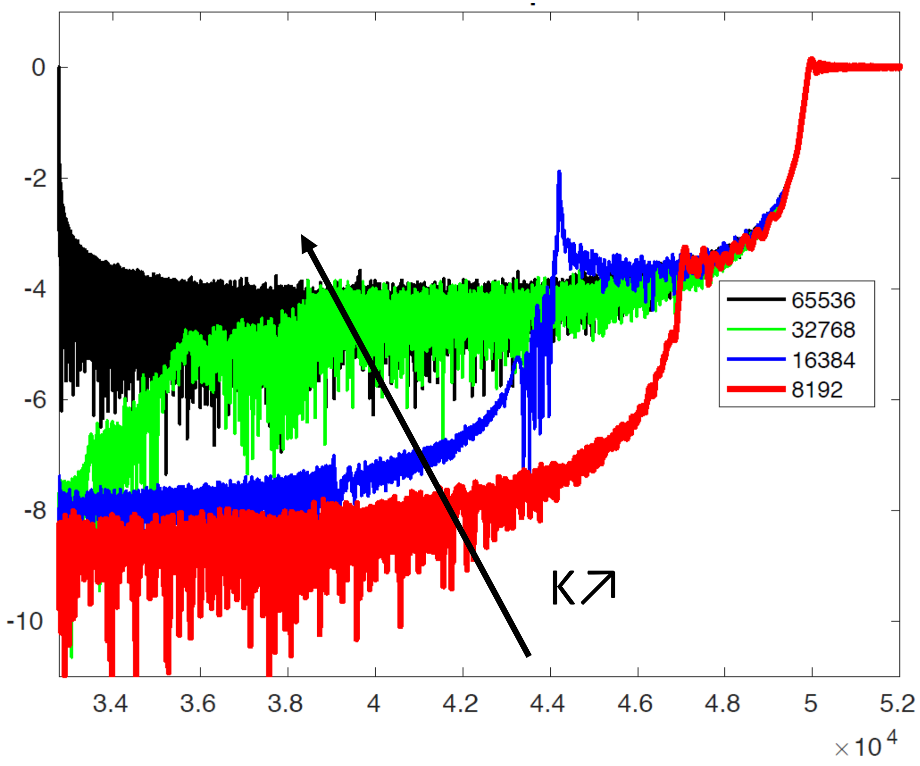

Reference curve (Hankel)

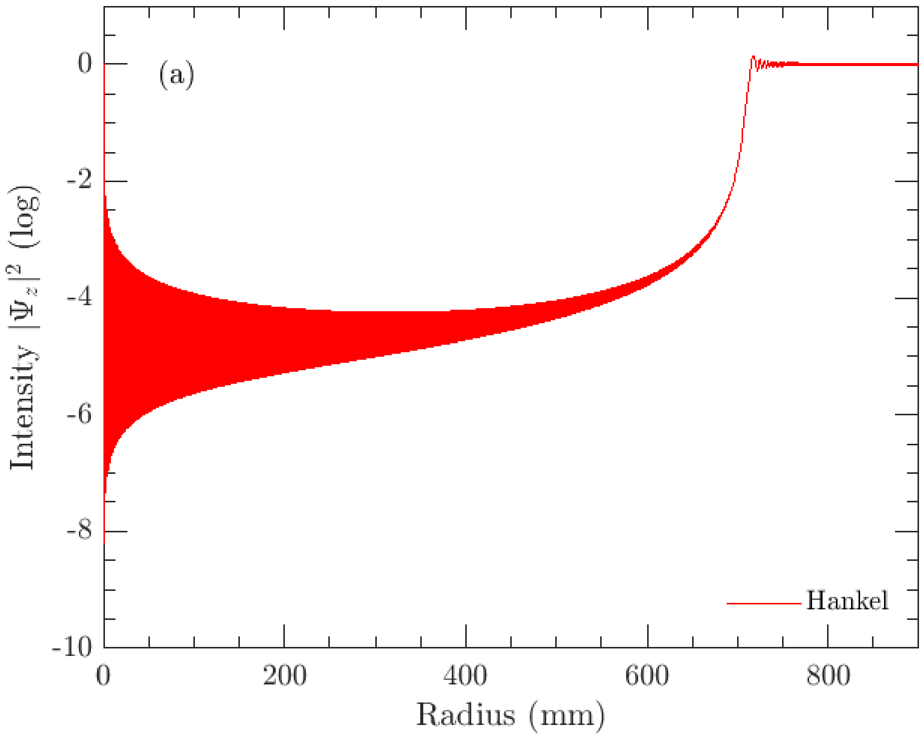

2D FFT technique

Very sensitive to numerical sampling: impact of sampling

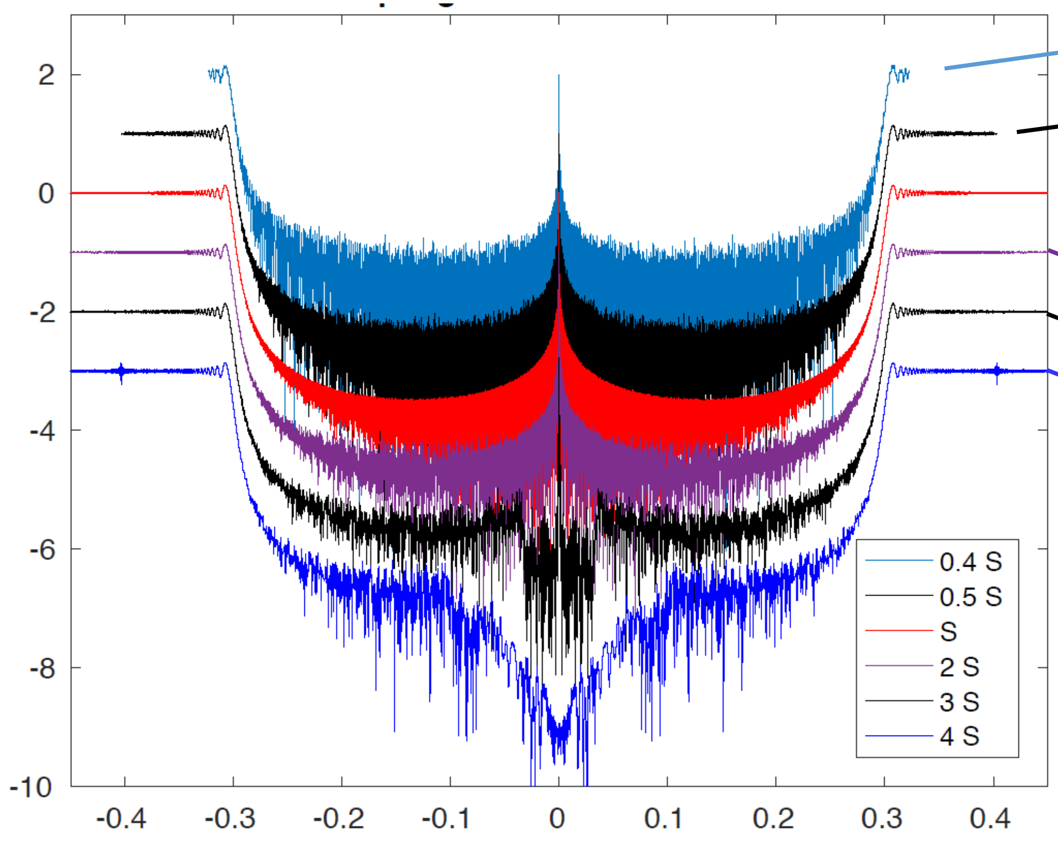

Sampling too small regarding Fresnel filter's condition

Sampling meeting the condition

Sampling too large to correctly sample the occulter

The Hankel transformation

Fourier wave optics formalism

Fresnel free-space propagation

Axis-symmetric (apodized) occulter

$$\Psi_z(x,y) = \big(1 - f(r)\big) \circledast \frac{1}{i\lambda z} \exp\left(\frac{i\pi}{\lambda z}(x^2 + y^2)\right)$$

$$\Psi_z(r) = \frac{\varphi_z(r)}{i\lambda z} \int_0^R 2\pi\rho \times f(\rho) \times \exp\left(\frac{i\pi\rho^2}{\lambda z}\right) \times J_0\left(\frac{2\pi\rho r}{\lambda z}\right) d\rho$$

Diffraction at z
Radial function

Radial apodization

Lommel series – decomposition into series (Aime, 2013)

The Hankel transformation

Fresnel free-space propagation

Axis-symmetric (apodized) occulter

$$\Psi_z(x,y) = \underbrace{\big(1 - f(r)\big)}_{\text{Radial apodization}} \circledast \frac{1}{i\lambda z} \exp\left(\frac{i\pi}{\lambda z}(x^2 + y^2)\right)$$

$$\Psi_z(r) = \frac{\varphi_z(r)}{i\lambda z} \int_0^R 2\pi\rho \times f(\rho) \times \exp\left(\frac{i\pi\rho^2}{\lambda z}\right) \times J_0\left(\frac{2\pi\rho r}{\lambda z}\right) d\rho$$

Lommel series: decomposition into series (Aime, 2013)

Vanderbei et al. approah

Based on Fresnel diffraction theory
For serrated or petal-shaped occulter, i.e. a periodic pattern by rotation

$$\Psi_z(r,\theta) = \Psi_z^{apod}(r) + \sum_{j=1}^{\infty} f_1(j, N_t) \times \int_0^{R+\Delta} f_2(j,\rho) \times J_{jN_t}\left(\frac{2\pi r\rho}{\lambda z}\right)\rho d\rho$$

In stellar coronagraphy:
$N_t \approx 20$, and very small working angles: j=1 dominates

In solar coronagraphy:
$N_t \approx 100 - 1000$, and large region (671mm): the computation is very heavy

Penumbra and Boivin radii

Penumbra for serrated occulters

Convolution of the diffraction intensity $|\Psi_z(x,y)|^2$ with the solar stenope image
Includes limb darkening function

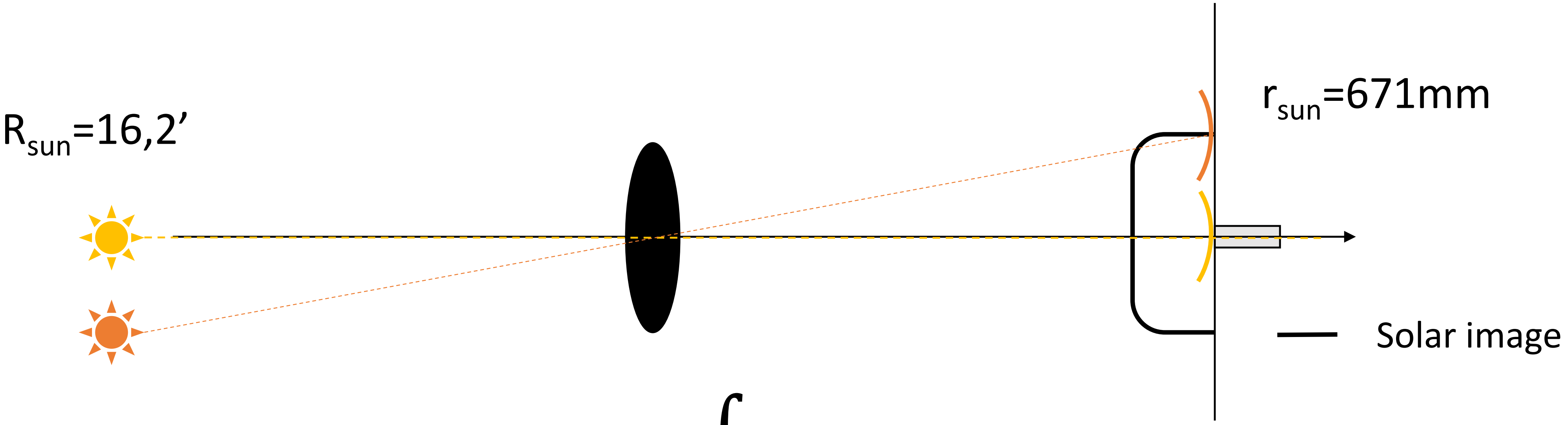

Penumbra: $\int_{\odot}$ Diffraction x Solar image

Penumbra for serrated occulters

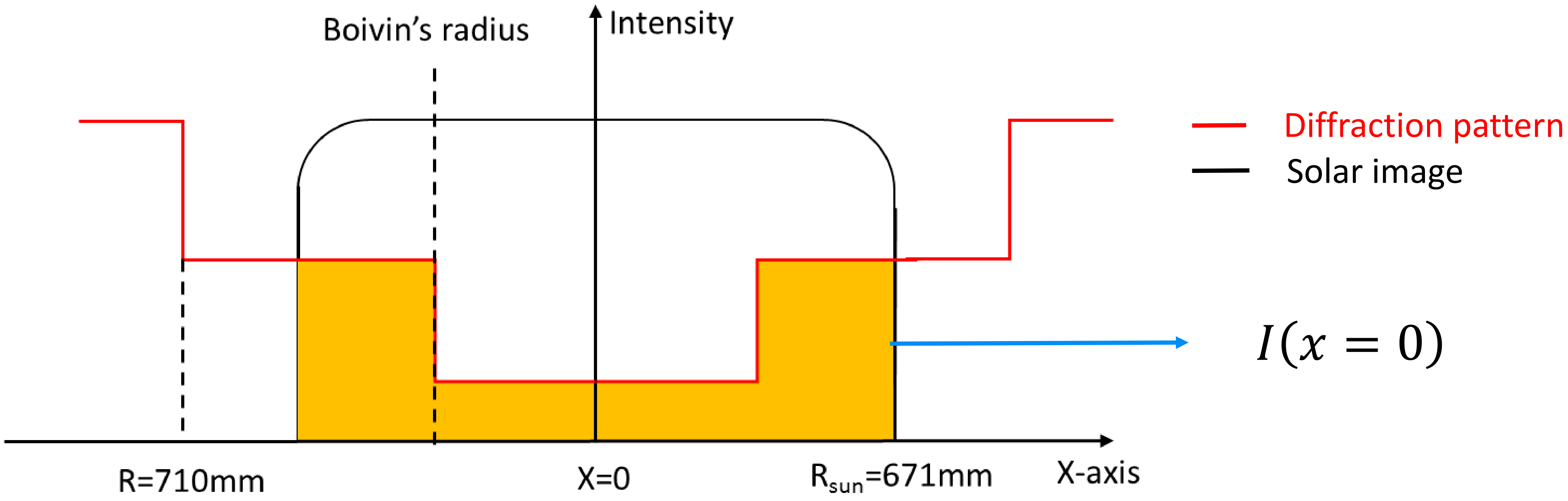

Penumbra for serrated occulters

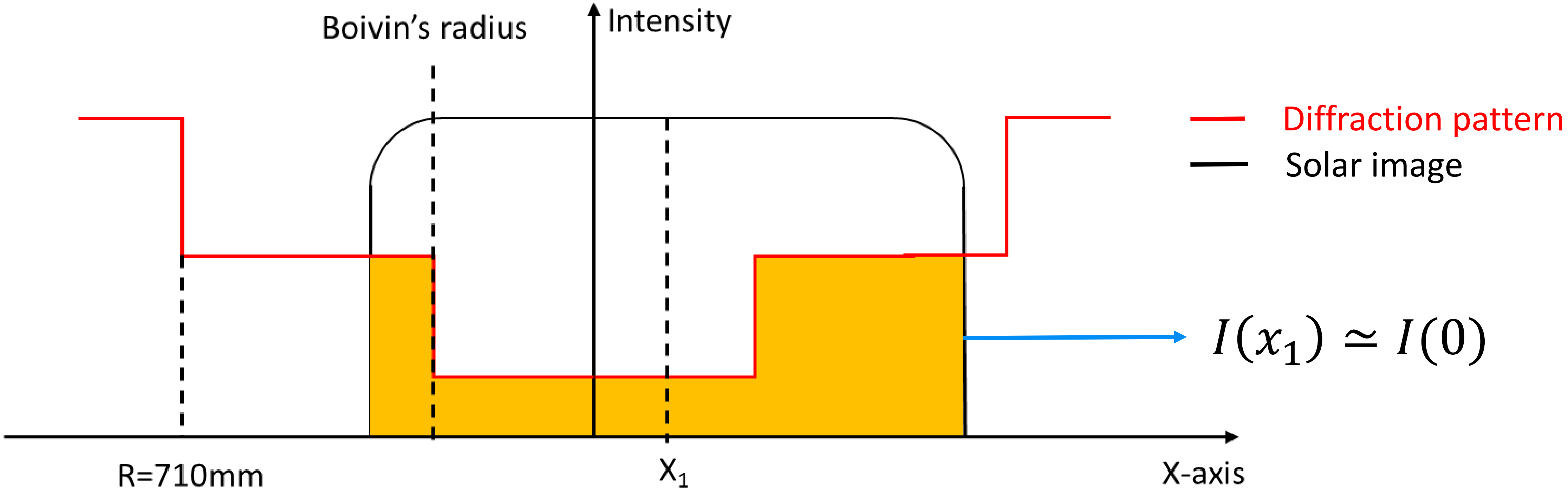

Penumbra for serrated occulters

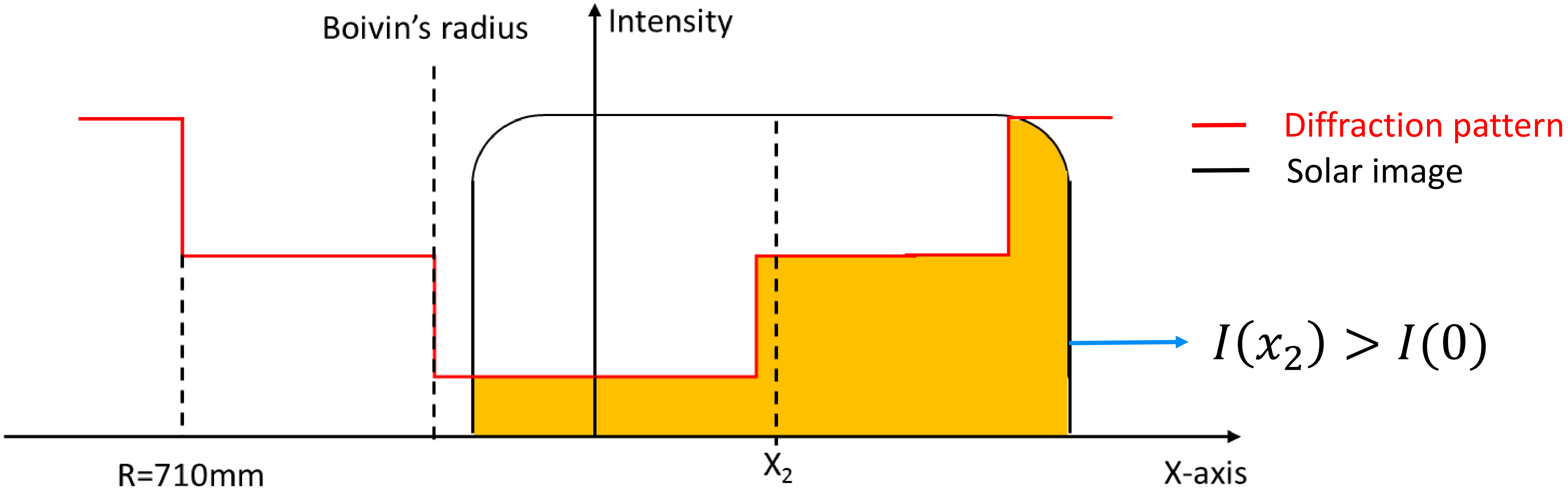

Penumbra for serrated occulters

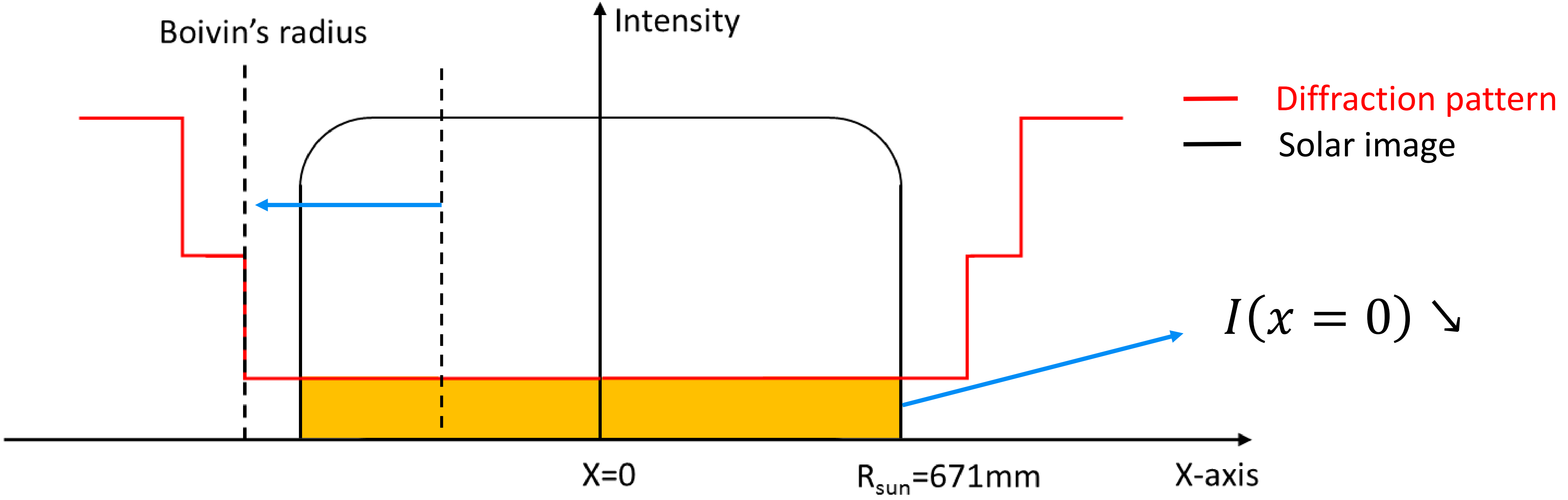

Penumbra for serrated occulters

We can predict the penumbra depth for serrated occulters:

The deepest umbra is achieved when:

$$\text{Boivin radius}(N_t, \Delta) > r_{sun}$$

The second parameter is the intensity level of the diffraction pattern

→ Large number of teeth preferred!